

A Reparameterized Discrete Diffusion Model for Text Generation

Lin Zheng¹ Jianbo Yuan² Lei Yu³ Lingpeng Kong¹

Abstract

This work studies discrete diffusion probabilistic models with applications to natural language generation. We derive an alternative yet equivalent formulation of the sampling from discrete diffusion processes and leverage this insight to develop a family of *reparameterized discrete diffusion models*. The derived generic framework is highly flexible, offers a fresh perspective of the generation process in discrete diffusion models, and features more effective training and decoding techniques. We conduct extensive experiments to evaluate the text generation capability of our model, demonstrating significant improvements over existing diffusion models.

1. Introduction

Diffusion-based generative models (Sohl-Dickstein et al., 2015; Ho et al., 2020; Song et al., 2021b), or diffusion models for short, have achieved remarkable progress and shown great success in generating high-quality and photo-realistic images (Ramesh et al., 2022; Saharia et al., 2022; Rombach et al., 2022; Balaji et al., 2022; Peebles & Xie, 2022). Researchers have successfully extended diffusion models to various data modalities beyond 2D images, including audio (Kong et al., 2021), video (Ho et al., 2022), as well as molecule generation (Hoogeboom et al., 2022b; Jo et al., 2022). There has also been a surge of interest in extending diffusion models to natural languages (Hoogeboom et al., 2021; Austin et al., 2021; Li et al., 2022; Dieleman et al., 2022). Diffusion-based language models are appealing in that the generation process is conducted in a non-autoregressive manner, which features in-parallel decoding by design and potentially leads to a faster runtime (Hoogeboom et al., 2021; Austin et al., 2021). In addition, due to the iterative reconstruction process in diffusion-based models, it is often possible to refine the previously generated texts (Savinov et al., 2022). As a result, compared with the

conventional auto-regressive models, diffusion-based language models are more flexible and attain better trade-offs between sampling quality and efficiency.

However, there are noticeably fewer success cases in employing diffusion models for large-scale text generation tasks. This is possibly due to the discrete nature of natural languages, while most conventional diffusion models focus on continuous-valued contents. To bridge the discrepancy, recent work aims at conducting the diffusion process over token embeddings so that the continuous diffusion models can be applied to discrete texts (Li et al., 2022; Gong et al., 2022; Strudel et al., 2022; Dieleman et al., 2022) or logits (Han et al., 2022; Richemond et al., 2022). Nevertheless, these approaches often require designing a well-crafted rounding scheme to convert the diffused continuous vectors to the actual discrete tokens. In addition, the existing continuous diffusion models require a sufficient number of sampling iterations to achieve the desired performance. This issue is exacerbated in the case of modeling texts, as the diffusing steps over text embeddings are hard to be translated to significant movements of token states due to the rounding quantization. This results in a considerably slower runtime than the auto-regressive language models. For example, a recent continuous diffusion model (DiffuSeq; Gong et al., 2022) runs several orders of magnitude slower than the auto-regressive baseline of a similar scale, as shown in Figure 3. Different from the above, another line of research focuses on constructing the diffusion process that directly operates on discrete state spaces (Sohl-Dickstein et al., 2015; Hoogeboom et al., 2021; Austin et al., 2021, see §2). However, they are relatively under-explored and often have inferior results in text generation.

In this work, we demonstrate that discrete diffusion models can serve as strong baselines for text generation. By re-examining the formulations, we observe that sampling from discrete diffusion models admits a novel yet equivalent *reparameterization* (§3). Specifically, starting with a completely noisy sequence, the sampling procedure in a discrete diffusion model is equivalent to the following *route-and-denoise* process where at each iteration, each token within the sequence is either denoised or reset to noisy states according to an underlying stochastic *routing* mechanism (§3.2). The router assigns the same probability to the decision for each token, processing the sequence in a uniform manner. Based

¹Department of Computer Science, The University of Hong Kong ²ByteDance Inc. ³DeepMind. Correspondence to: Lin Zheng <linzheng@connect.hku.hk>.

on this insight, we propose **Reparameterized Discrete diffusion Models** (RDMs), a new family of models that respects the reparameterization and formulates the routing process explicitly. RDMs enjoy appealing properties for both training (§4.2) and sampling (§4.3): (1) *Simplified training*. We demonstrate that the training objective for RDMs can be reduced to a re-weighted standard cross-entropy loss. Furthermore, the loss objective is invariant to different routing probabilities up to reweighting, indicating that the large family of RDMs with distinct routing processes can be trained with the same surrogate objective; (2) *Flexible sampling*. Thanks to the shared objective, the sampling process is highly flexible and allows more expressive routing processes. In particular, we develop an adaptive routing strategy that routes tokens to the denoised state only if the router outputs high scores, as opposed to processing all the tokens uniformly. Equipped with such training and decoding schemes, we demonstrate that RDMs significantly improve vanilla discrete diffusion models across several standard text generation benchmarks (§5). They also achieve much better performance than the continuous diffusion models while running several orders faster.¹

2. Background

Suppose the data $\mathbf{x}_0 \sim p_{\text{data}}(\mathbf{x}_0)$ is a discrete random variable with K possible outcomes. To ease notation, we represent discrete variables as one-hot vectors in $\{0, 1\}^K$, which is 0 everywhere except that the entry corresponding to the current state is 1. Discrete diffusion probabilistic models (Sohl-Dickstein et al., 2015; Hoogeboom et al., 2021; Austin et al., 2021) are usually defined as a class of latent variable models characterized by a forward and backward process. The *forward* process aims to gradually transform input data to some noise distribution q_{noise} through T intermediate latent variables $\mathbf{x}_1, \dots, \mathbf{x}_T \in \{0, 1\}^K$, with the forward transition $q(\mathbf{x}_t | \mathbf{x}_{t-1}) = \beta_t \mathbf{x}_{t-1} + (1 - \beta_t) q_{\text{noise}}$. In this case, the distribution $q(\mathbf{x}_t | \mathbf{x}_0)$ is available in closed form,

$$q(\mathbf{x}_t | \mathbf{x}_0) = \alpha_t \mathbf{x}_{t-1} + (1 - \alpha_t) q_{\text{noise}}, \quad (1)$$

where $\alpha_t := \prod_{i=1}^t \beta_i$ is specified to decrease from 1 to 0 w.r.t. t . The noise distribution q_{noise} characterizes different diffusion processes; for example, **multinomial diffusion** (Hoogeboom et al., 2021) adopts a uniform noise distribution over the vocabulary $\{1, 2, \dots, K\}$; alternatively, **absorbing diffusion** specifies q_{noise} to be a point mass with all of the probability on an absorbing state (Austin et al., 2021).

The *backward* process $q(\mathbf{x}_{t-1} | \mathbf{x}_t)$ is the key ingredient for diffusion-based generative modeling, based on which we can start with unstructured noise $\mathbf{x}_T \sim q_{\text{noise}}$ and perform ancestral sampling $\mathbf{x}_{t-1} \sim q(\mathbf{x}_{t-1} | \mathbf{x}_t)$ to obtain new

¹Our code and models are available at <https://github.com/hkunlp/reparam-discrete-diffusion>

draws from $p_{\text{data}}(\mathbf{x}_0)$. Unfortunately, the backward transition $q(\mathbf{x}_{t-1} | \mathbf{x}_t)$ is mostly intractable due to the marginalization over the entire data distribution. Therefore, we resort to approximating it with a parameterized distribution $p_{\theta}(\mathbf{x}_{t-1} | \mathbf{x}_t)$ at each step t . This results in a generative model $p_{\theta}(\mathbf{x}_0, \mathbf{x}_1, \dots, \mathbf{x}_T) = p_{\theta}(\mathbf{x}_T) \prod_{t=1}^T p_{\theta}(\mathbf{x}_{t-1} | \mathbf{x}_t)$, which can be trained by maximizing the evidence lower bound (ELBO) of $\log p_{\theta}(\mathbf{x}_0)$,

$$\log p_{\theta}(\mathbf{x}_0) \geq \mathcal{L}_1(\theta) - \sum_{t=2}^T \mathcal{L}_t(\theta) + \text{const.},$$

with $\mathcal{L}_1(\theta) := \mathbb{E}_{q(\mathbf{x}_1 | \mathbf{x}_0)} [\log p_{\theta}(\mathbf{x}_0 | \mathbf{x}_1)]$ and $\mathcal{L}_t(\theta) := \mathbb{E}_{q(\mathbf{x}_t | \mathbf{x}_0)} [\text{KL}(q(\mathbf{x}_{t-1} | \mathbf{x}_t, \mathbf{x}_0) \| p_{\theta}(\mathbf{x}_{t-1} | \mathbf{x}_t))]$. The ELBO decomposes into a sum of KL divergences between the *conditional backward transition* $q(\mathbf{x}_{t-1} | \mathbf{x}_t, \mathbf{x}_0)$ and $p_{\theta}(\mathbf{x}_{t-1} | \mathbf{x}_t)$ at each time step t . Note that $q(\mathbf{x}_{t-1} | \mathbf{x}_t, \mathbf{x}_0) \propto q(\mathbf{x}_t | \mathbf{x}_{t-1}) q(\mathbf{x}_{t-1} | \mathbf{x}_0)$ can be calculated analytically for most discrete diffusion models. To define the distribution $p_{\theta}(\mathbf{x}_{t-1} | \mathbf{x}_t)$, previous work (Hoogeboom et al., 2021) suggests that it can be parameterized in a similar manner to $q(\mathbf{x}_{t-1} | \mathbf{x}_t, \mathbf{x}_0)$ by letting $p_{\theta}(\mathbf{x}_{t-1} | \mathbf{x}_t) = q(\mathbf{x}_{t-1} | \mathbf{x}_t, f(\mathbf{x}_t; \theta))$, where a neural network $f(\mathbf{x}_t; \theta)$ is adopted to predict \mathbf{x}_0 . Typically $f(\mathbf{x}_t; \theta) \in (0, 1)^K$ is the model output normalized by a softmax function, representing the probability vector for each token. A more detailed review and relevant derivations about discrete diffusion models are provided in Appendix A.

3. Reparameterizing Backward Processes

This section presents an in-depth study of discrete diffusion probabilistic models. We derive an alternative formulation for the backward process (§3.1) and devise a reparameterized sampling scheme (§3.2), which paves the way for a more generic family of discrete diffusion models (§4).

3.1. An Alternative Backward Formulation

We first elaborate on how the conditional backward transition of existing discrete diffusion models can be written in a more compact formulation (see Appendix B for the proof).

Proposition 3.1. *Let the forward transition of discrete diffusion models be $q(\mathbf{x}_t | \mathbf{x}_{t-1}) = \beta_t \mathbf{x}_{t-1} + (1 - \beta_t) q_{\text{noise}}$. Then the conditional backward transition distribution given \mathbf{x}_0 , $q(\mathbf{x}_{t-1} | \mathbf{x}_t, \mathbf{x}_0)$, can be equivalently written as*

$$q(\mathbf{x}_{t-1} | \mathbf{x}_t, \mathbf{x}_0) = \begin{cases} \lambda_{t-1}^{(1)} \mathbf{x}_t + \left(1 - \lambda_{t-1}^{(1)}\right) q_{\text{noise}}, & \text{if } \mathbf{x}_t = \mathbf{x}_0 \\ \lambda_{t-1}^{(2)} \mathbf{x}_0 + \left(1 - \lambda_{t-1}^{(2)}\right) q_{\text{noise}}(\mathbf{x}_t), & \text{if } \mathbf{x}_t \neq \mathbf{x}_0. \end{cases} \quad (2)$$

Here $q_{\text{noise}}(\mathbf{x}_t) = \beta_t \mathbf{x}_t + (1 - \beta_t) q_{\text{noise}}$ denotes a noise distribution that interpolates between \mathbf{x}_t and q_{noise} , $\lambda_{t-1}^{(1)} :=$

$1 - \frac{(1-\beta_t)(1-\alpha_{t-1})q_{\text{noise}}(\mathbf{u}=\mathbf{x}_t)}{\alpha_t + (1-\alpha_t)q_{\text{noise}}(\mathbf{u}=\mathbf{x}_t)}$, and $\lambda_{t-1}^{(2)} := \frac{\alpha_{t-1}-\alpha_t}{1-\alpha_t}$, where $q_{\text{noise}}(\mathbf{u}=\mathbf{x}_t)$ is the probability of the noise equal to \mathbf{x}_t .

Intuitively, Equation 2 reveals that the main mechanism of the backward process is to shuttle discrete tokens between fully noisy states and the ground truth state \mathbf{x}_0 , conditioned on the equality of \mathbf{x}_t and \mathbf{x}_0 . If $\mathbf{x}_t = \mathbf{x}_0$, the current token state is possibly noise-free, and the model either remains noise-free by copying the state $\mathbf{x}_{t-1} \leftarrow \mathbf{x}_t$, or resets the state to the noise. If $\mathbf{x}_t \neq \mathbf{x}_0$, the current state is considered noisy, and the model opts to denoise \mathbf{x}_t to \mathbf{x}_0 or remains noisy otherwise. The probability of moving noisy tokens to ground truth states or turning denoised tokens back to noise is governed by $\lambda_{t-1}^{(2)}$ and $1 - \lambda_{t-1}^{(1)}$, respectively.

3.2. Reparameterized Sampling

Next, we demonstrate that sampling from the backward transition can be conducted via an augmented path, leading to our full reparameterization. We make use of the simple fact that the mixture distribution in Equation 2 can be sampled in two steps: first, randomly select a component according to their weight, and then sample from the corresponding component distribution. Concisely, we have

$$\begin{aligned} b_t &= \mathbf{1}_{\mathbf{x}_t = \mathbf{x}_0} \\ v_{t-1}^{(1)} &\sim \text{Bernoulli}\left(\lambda_{t-1}^{(1)}\right), \quad \mathbf{u}_t^{(1)} \sim q_{\text{noise}} \\ v_{t-1}^{(2)} &\sim \text{Bernoulli}\left(\lambda_{t-1}^{(2)}\right), \quad \mathbf{u}_t^{(2)} \sim q_{\text{noise}}(\mathbf{x}_t) \\ \mathbf{x}_{t-1} &= b_t \left[v_{t-1}^{(1)} \mathbf{x}_t + \left(1 - v_{t-1}^{(1)}\right) \mathbf{u}_t^{(1)} \right] + \\ &\quad (1 - b_t) \left[v_{t-1}^{(2)} \mathbf{x}_0 + \left(1 - v_{t-1}^{(2)}\right) \mathbf{u}_t^{(2)} \right]. \quad (3) \end{aligned}$$

To simplify the notation, we denote $\mathbf{v}_{t-1} := [v_{t-1}^{(1)}, v_{t-1}^{(2)}]$ and $\lambda_{t-1} := [\lambda_{t-1}^{(1)}, \lambda_{t-1}^{(2)}]$. This reparameterized backward transition highlights an underlying *routing* mechanism, where the model routes tokens to different distributions according to \mathbf{v}_{t-1} : given b_t that discriminates which tokens are currently noisy, $v_{t-1}^{(1)}$ selects and denoises noisy tokens to recover the ground truth \mathbf{x}_0 , while $v_{t-1}^{(2)}$ determines which denoised tokens revert to the noisy state.

4. Reparameterized Discrete Diffusion Models

In this section, we introduce our proposed diffusion models that reflect the reparameterization (§4.1), which imply effective training (§4.2) and sampling (§4.3) algorithms.

4.1. A Joint Diffusion Model

The routing mechanism above works in a latent manner; that is, it is only active during the sampling process but

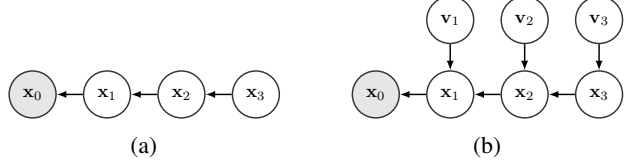


Figure 1: The graphical model diagram describing the backward transition process of (a) conventional discrete diffusion, and (b) our reparameterized discrete diffusion models.

marginalized when advancing the distribution of \mathbf{x}_{t-1} . To fully utilize the potential of the developed reparameterization, we propose to elevate the latent routing mechanism to the formulation explicitly and model the *joint* distribution over both \mathbf{x} and \mathbf{v} ,

$$\begin{aligned} \mathbf{x}_{t-1}, \mathbf{v}_{t-1} &\sim q(\mathbf{x}_{t-1}, \mathbf{v}_{t-1} | \mathbf{x}_t, \mathbf{x}_0) \\ q(\mathbf{v}_{t-1} | \mathbf{x}_t, \mathbf{x}_0) &= q(\mathbf{v}_{t-1}) = \text{Bernoulli}(\boldsymbol{\lambda}) \\ q(\mathbf{x}_{t-1} | \mathbf{v}_{t-1}, \mathbf{x}_t, \mathbf{x}_0) &= \\ \begin{cases} v_{t-1}^{(1)} \mathbf{x}_t + \left(1 - v_{t-1}^{(1)}\right) q_{\text{noise}}, & \text{if } \mathbf{x}_t = \mathbf{x}_0 \\ v_{t-1}^{(2)} \mathbf{x}_0 + \left(1 - v_{t-1}^{(2)}\right) q_{\text{noise}}(\mathbf{x}_t), & \text{if } \mathbf{x}_t \neq \mathbf{x}_0. \end{cases} \quad (4) \end{aligned}$$

This can be considered as a standard discrete diffusion model augmented with step-wise routing indicators $\{\mathbf{v}_{t-1}\}_{t=1}^T$ (see the graphical model diagram in Figure 1). It closely relates to the conventional formulation (Equation 2) in that the original backward process amounts to marginalizing out \mathbf{v}_{t-1} at each time step: $q(\mathbf{x}_{t-1} | \mathbf{x}_t, \mathbf{x}_0) = \mathbb{E}_{q(\mathbf{v}_{t-1})} [q(\mathbf{x}_{t-1} | \mathbf{v}_{t-1}, \mathbf{x}_t, \mathbf{x}_0)]$. Since the distribution over \mathbf{v}_{t-1} is also taken into account, this joint diffusion model offers improved flexibility and expressiveness. We refer to this class of models as *reparameterized discrete diffusion models* (RDMs), as it yields an equivalent sampling process to the original formulation but via a reparameterized path.

4.2. Training

Similar to previous diffusion models (§2), we define a joint generative process $p_{\theta}(\mathbf{x}_{t-1}, \mathbf{v}_{t-1} | \mathbf{x}_t)$ and optimize the ELBO via the following factorization,

$$\begin{aligned} \log p(\mathbf{x}_0) &\geq \mathbb{E}_{q(\mathbf{x}_{1:T}, \mathbf{v}_{1:T} | \mathbf{x}_0)} \left[\log \frac{p_{\theta}(\mathbf{x}_0, \mathbf{x}_{1:T}, \mathbf{v}_{1:T})}{q(\mathbf{x}_{1:T}, \mathbf{v}_{1:T} | \mathbf{x}_0)} \right] \\ &:= \mathcal{L}_1(\boldsymbol{\theta}) - \sum_{t=2}^T \mathcal{L}_t(\boldsymbol{\theta}) + \text{const.} \end{aligned}$$

Following standard practices in diffusion models (Hoogboom et al., 2021; Austin et al., 2021), we randomly sample a time step t and optimize $\boldsymbol{\theta}$ with respect to $\mathcal{L}_t(\boldsymbol{\theta})$. In our case, $\mathcal{L}_1(\boldsymbol{\theta}) = \mathbb{E}_{q(\mathbf{x}_1 | \mathbf{x}_0)} [\log p_{\theta}(\mathbf{x}_0 | \mathbf{x}_1)]$; for $t > 1$, \mathcal{L}_t decomposes into a sum of two KL divergences over \mathbf{v}_{t-1} and

\mathbf{x}_{t-1} respectively,

$$\begin{aligned}\mathcal{L}_t(\boldsymbol{\theta}) = & \mathbb{E}_{q(\mathbf{x}_t|\mathbf{x}_0)} [\text{KL}(q(\mathbf{v}_{t-1}) \parallel p_{\boldsymbol{\theta}}(\mathbf{v}_{t-1}))] + \\ & \mathbb{E} [\text{KL}(q(\mathbf{x}_{t-1}|\mathbf{v}_{t-1}, \mathbf{x}_t, \mathbf{x}_0) \parallel p_{\boldsymbol{\theta}}(\mathbf{x}_{t-1}|\mathbf{v}_{t-1}, \mathbf{x}_t))],\end{aligned}\quad (5)$$

where the second expectation is with respect to $q(\mathbf{x}_t|\mathbf{x}_0)q(\mathbf{v}_{t-1})$. The full derivation is in Appendix C.

Parameterization. The decomposition in Equation 5 suggests parameterizing each conditional of $p_{\boldsymbol{\theta}}(\mathbf{x}_{t-1}, \mathbf{v}_{t-1}|\mathbf{x}_t) = p_{\boldsymbol{\theta}}(\mathbf{x}_{t-1}|\mathbf{v}_{t-1}, \mathbf{x}_t)p_{\boldsymbol{\theta}}(\mathbf{v}_{t-1}|\mathbf{x}_t)$ separately. To simplify the model representation, we constrain $p_{\boldsymbol{\theta}}(\mathbf{v}_{t-1}|\mathbf{x}_t)$ to be the same as $q(\mathbf{v}_{t-1})$ so that the first KL term is equal to zero. In terms of $p_{\boldsymbol{\theta}}(\mathbf{x}_{t-1}|\mathbf{v}_{t-1}, \mathbf{x}_t)$, it needs to approximate $q(\mathbf{x}_{t-1}|\mathbf{v}_{t-1}, \mathbf{x}_t, \mathbf{x}_0)$ for both \mathbf{x}_0 and $b_t = \mathbf{1}_{\mathbf{x}_t=\mathbf{x}_0}$. For the former, we approximate \mathbf{x}_0 with a neural network output $f(\mathbf{x}_t; \boldsymbol{\theta})$ (§2); for the latter, it is circumvented via a *teacher-forcing* approach. We leverage the fact that $b_t = \mathbf{1}_{\mathbf{x}_t=\mathbf{x}_0}$ is readily available during training and plug the oracle into $p_{\boldsymbol{\theta}}(\mathbf{x}_{t-1}|\mathbf{v}_{t-1}, \mathbf{x}_t)$, which works well empirically and yields interesting implications as presented below.

Simplified Training Objectives. So far, we mainly consider the case of a single token. We now slightly abuse the term and denote a sequence of tokens at t -th time step as $\mathbf{x}_{t,1:N} := \{\mathbf{x}_{t,n}\}_{n=1}^N$, where $\mathbf{x}_{t,n}$ is the n -th token and N is the sequence length.² We also assume distributions factorize over each token. We show that the sequence-level training objective $\mathcal{L}_t(\boldsymbol{\theta})$ can be reduced to a surprisingly simple expression (see Appendix D for the proof).

Proposition 4.1. *The loss objective $\mathcal{L}_t(\boldsymbol{\theta})$ for sequence $\mathbf{x}_{t,1:N}$ at the t -th step can be reduced to the form*

$$\mathcal{L}_t(\boldsymbol{\theta}) = \mathbb{E} \left[-\lambda_{t-1}^{(2)} \sum_{n=1}^N (1-b_{t,n}) \mathbf{x}_{0,n}^\top \log f(\mathbf{x}_{t,n}; \boldsymbol{\theta}) \right], \quad (6)$$

where the expectation above is calculated with respect to $p_{\text{data}}(\mathbf{x}_{0,1:N}) \prod_{n=1}^N q(\mathbf{x}_{t,n}|\mathbf{x}_{0,n})$.

Remark 4.2. The resulting loss objective Equation 6 is invariant to the distribution $q(\mathbf{v}_{t-1})$ up to reweighting.

Based on this result, training RDMs is equivalent to optimizing the standard *multi-class cross-entropy* loss function, which is evaluated over noisy tokens and weighted by $\lambda_{t-1}^{(2)} = \mathbb{E} [\mathbf{v}_{t-1}^{(2)}]$. This formulation is conceptually simpler than that of the original discrete diffusion, which requires evaluating the KL divergence between two complicated categoricals (Hoogeboom et al., 2021). Besides, this formulation establishes the discrete analog of *reweighting*

²We use \mathbf{x}_t and $\mathbf{x}_{t,n}$ interchangeably to represent a single token when there is no ambiguity; this also applies to other variables such as \mathbf{x}_t , etc.

training strategies, which are recognized as common practices for training continuous-domain diffusion models (Ho et al., 2020; Nichol & Dhariwal, 2021; Vahdat et al., 2021; Karras et al., 2022). In particular, we can adjust the weight $\lambda_{t-1}^{(2)}$ to reweigh the cross-entropy function so that it is more amenable for training.

More importantly, in Remark 4.2, we demonstrate that different $q(\mathbf{v}_{t-1})$ would lead to the same shared objective except for the weight $\lambda_{t-1}^{(2)} = \mathbb{E} [\mathbf{v}_{t-1}^{(2)}]$. This makes it possible to train the neural network with one amenable distribution of \mathbf{v}_{t-1} but share the trained model for sampling among a broad family of diffusion processes indexed by $q(\mathbf{v}_{t-1})$.

4.3. Sampling

Sampling from discrete diffusion processes usually starts with a sequence comprising only noisy tokens and proceeds by drawing $\mathbf{x}_{t-1}, \mathbf{v}_{t-1} \sim p_{\boldsymbol{\theta}}(\mathbf{x}_{t-1}, \mathbf{v}_{t-1}|\mathbf{x}_t)$ at each step.

Generating \mathbf{v}_{t-1} . A naïve approach of generating \mathbf{v}_{t-1} is drawing $\mathbf{v}_{t-1} \sim \text{Bernoulli}(\boldsymbol{\lambda})$. However, this assigns the same probability $\boldsymbol{\lambda}_{t-1}$ to all tokens. Since the role of \mathbf{v}_{t-1} is to route tokens to noisy or denoised states, it is expected to be discriminative in processing tokens rather than being blind. Fortunately, Remark 4.2 allows us to employ a more discriminative approach, where a token is denoised only when it receives high scores from the neural network (Ghazvininejad et al., 2019; Savinov et al., 2022; Chang et al., 2022). At each time step, we first feed a noisy sequence $\mathbf{x}_{t,1:N}$ into the neural network and collect the output $f(\mathbf{x}_{t,n}; \boldsymbol{\theta})$ for each token n . Since $f(\mathbf{x}_{t,n}; \boldsymbol{\theta}) \in (0, 1)^K$ is the probability vector, we take the maximum value as the score for each token $s_{t,n} := \max_{1 \leq j \leq K} f_j(\mathbf{x}_{t,n}; \boldsymbol{\theta})$. After that, we fetch tokens with the k largest scores and only set $\mathbf{v}_{t-1,n}$ at these positions to 1. Formally,

$$\mathcal{P}_{t-1} = \arg \text{topk} \{s_{t,n}\}_{n=1}^N, \quad \mathbf{v}_{t-1,n}^{(i)} = \mathbf{1}_{n \in \mathcal{P}_{t-1}}, \quad (7)$$

where $i = 1$ if $b_{t,n} = 1$ and $i = 2$ otherwise. This strategy is more informative, as the router can compare token scores to determine their states. Although \mathbf{v}_{t-1} is defined as a function of model scores and its explicit probability distribution is possibly intractable, the usage of such adaptive mechanism is well justified by Remark 4.2, since the diffusion model corresponding to this implicit distribution can also be trained with the shared surrogate objective.

Recursive Computation for b_t . Another challenge during decoding stems from the computation $b_t = \mathbf{1}_{\mathbf{x}_t=\mathbf{x}_0}$, which is intractable since we do not have access to the ground truth information \mathbf{x}_0 as in training. We capitalize on an observation that a recursive computation can circumvent the requirement of \mathbf{x}_0 , which derives b_{t-1} based on the

Algorithm 1 Training RDMs

Input: neural network $f(\cdot; \theta)$, data distribution $p_{\text{data}}(\mathbf{x}_{0,1:N})$, and a custom reweighting scalar λ_{t-1} .
Output: model parameters θ .

repeat

- Draw $\mathbf{x}_{0,1:N} \sim p_{\text{data}}(\mathbf{x}_{0,1:N})$;
- Draw $t \in \text{Uniform}(\{1, \dots, T\})$;
- for** $n = 1, 2, \dots, N$ **do**

 - Draw $\mathbf{x}_{t,n} \sim q(\mathbf{x}_{t,n} | \mathbf{x}_{0,n})$;
 - Let $b_{t,n} = \mathbf{1}_{\mathbf{x}_{t,n} = \mathbf{x}_{0,n}}$;

- end for**
- $\mathcal{L}(\theta) = -\lambda_{t-1} \sum_{n=1}^N (1 - b_{t,n}) \mathbf{x}_{0,n}^\top \log f(\mathbf{x}_{t,n}; \theta)$;
- Minimize $\mathcal{L}(\theta)$ with respect to θ ;
- until** converged

functionality of \mathbf{v}_t as follows,

$$b_{t-1} = (b_t \wedge v_{t-1}^{(1)}) \vee v_{t-1}^{(2)}, \quad (8)$$

where $b_T = 0$ for all tokens. Concisely, b_t implies a frontier set that stores the denoised tokens up to the previous iteration. At the current iteration, we add new tokens to the set if $v_{t-1}^{(2)} = 1$ and remove elements from the set if the corresponding $v_{t-1}^{(1)} = 0$. The updated set is then read out to form b_{t-1} .³ Note that the update does not add extra computational costs. Equipped with these results, we can efficiently execute the sampling algorithm without difficulties.

4.4. Implementation

Algorithms 1 and 2 list the full pseudo-codes for training and sampling of RDMs, respectively. Note that the loop over the sequence length N is computed in parallel. The developed formulation of RDMs offers great flexibility for both training and sampling. For instance, we can pass a custom λ_{t-1} to reweigh the loss for training, similar to continuous diffusion models. Besides, the denoised token states $\tilde{\mathbf{x}}_0$ during decoding can be obtained in various ways, such as sampling with annealed temperatures or simply taking the arg max of $f(\mathbf{x}_{t,n}; \theta)$. Please refer to Appendix E for the full implementation details.

5. Experiments

We conduct experiments on various text generation benchmarks to evaluate our model. Our implementation for all tasks is based on FairSeq toolkit (Ott et al., 2019), and a detailed experimental setup can be found in Appendix E.

³Technically, for certain noise distributions, the logic operation \wedge and \vee should be noisy since they should compensate for the possibility that noises drawn from q_{noise} can also coincide with \mathbf{x}_0 ; however, for most diffusion processes considered in this work, such probability is so small that it can be safely ignored.

Algorithm 2 Sampling from RDMs

Input: trained network parameters θ and temperature τ .
Output: generated sample \mathbf{x}_0 .

for $n = 1, 2, \dots, N$ **do**

- Initialize $\mathbf{x}_{T,n} \sim q_{\text{noise}}$;
- Initialize $b_{T,n} = 0$;

end for

for $t = T, \dots, 1$ **do**

- for** $n = 1, 2, \dots, N$ **do**

 - Draw $\tilde{\mathbf{x}}_{0,n} \sim \text{Categorical}(f(\mathbf{x}_{t,n}; \theta) / \tau)$;
 - Generate $\mathbf{v}_{t-1,n}$ according to Equation 7;
 - $b_{t-1,n} = b_{t,n} \wedge v_{t-1,n}^{(1)} \vee v_{t-1,n}^{(2)}$;
 - if** $b_{t-1,n} = 1$ **then**

 - Draw $\mathbf{u}_{t,n}^{(1)} \sim q_{\text{noise}}(\mathbf{x}_{t,n})$;
 - $\mathbf{x}_{t-1,n} = v_{t-1,n}^{(1)} \mathbf{x}_{t,n} + (1 - v_{t-1,n}^{(1)}) \mathbf{u}_{t,n}^{(1)}$;

 - else**

 - Draw $\mathbf{u}_{t,n}^{(2)} \sim q_{\text{noise}}(\mathbf{x}_{t,n})$;
 - $\mathbf{x}_{t-1,n} = v_{t-1,n}^{(2)} \tilde{\mathbf{x}}_{0,n} + (1 - v_{t-1,n}^{(2)}) \mathbf{u}_{t,n}^{(2)}$;

 - end if**

end for

end for

Return $\mathbf{x}_{0,1:N}$.

5.1. Machine Translation

Setup. For experiments on machine translation, we consider three standard benchmarks:

- IWSLT14 DE-EN (Cettolo et al., 2014), which contains around 160K/7K/7K sentence pairs for training, validation, and testing, respectively. We build a joint vocabulary for the source and target language, resulting in 10152 Byte Pair Encoding (BPE; Sennrich et al., 2016) types.
- WMT14 EN-DE (Bojar et al., 2014) dataset consists of around 4.0M/3K/3K training/validation/testing pairs. The preprocessing follows Ghazvininejad et al. (2019) and yields a shared vocabulary with 40624 BPE types;
- WMT16 EN-RO (Bojar et al., 2016). We use the same data split from Lee et al. (2018) that comprises around 610K/2K/2K pairs. The vocabulary is shared between the source and target sides with 34976 joint BPE types.

For all translation tasks, we operate on original data and do *not* adopt knowledge distillation (Kim & Rush, 2016; Gu et al., 2018) that replaces the target side of training data with outputs generated by a pre-trained autoregressive Transformer.

Results. As seen from Table 1, existing discrete diffusion models usually perform badly on the translation task and do not scale well for large-sized datasets. In particular,

multinomial diffusion achieves worse translation quality albeit with more iterations and fails to decode decently on WMT14 EN-DE dataset. The proposed reparameterization yields significant performance boosts (about 3~20 BLEU improvements) on both absorbing and multinomial diffusion across all datasets and iteration steps. We also observe that the performance gain is much more significant for multinomial diffusion, which is possibly due to the fix of its degenerated behavior (more details are in §5.4). Our approach effectively scales these diffusion models to larger datasets and achieves promising results even competitive with auto-regressive baselines. Besides, RDMs can achieve significantly better performance than a continuous diffusion model CDCD (Dieleman et al., 2022) while running with more than 8 \times fewer iterations.

5.2. Question Generation and Paraphrasing

Setup. We also test the performance of our model on general sequence-to-sequence generation tasks, following Gong et al. (2022). Due to the limited computation budget, we mainly consider the question generation and paraphrasing tasks using the same pre-processed data split as in Gong et al. (2022):

- Question Generation (QG) with the Quasar-T dataset (Dhingra et al., 2017), containing around 117K/2K/10K pairs for training/validation/testing, respectively.
- Paraphrasing with Quora Question Pairs (QQP). This dataset comprises around 145K/2K/2.5K training/validation/testing question pairs.

For both QG and QQP tasks, we use the same WordPiece tokenization as in BERT (Devlin et al., 2019) and obtain a vocabulary of size 30522.

Results. We report the comparisons among discrete diffusion, continuous diffusion, and auto-regressive baselines in Table 2. We observe that either variant of RDMs not only improves their vanilla counterparts by a large margin but also outperforms the strong continuous diffusion baseline DiffuSeq as well as various auto-regressive baselines across several evaluation metrics. Besides, DiffuSeq needs 2000 steps to finish the decoding, while RDMs can produce higher-quality samples with 10 iterations, reducing runtime by over 200 \times . This implies that RDMs can attain a much better trade-off between generation quality and runtime. In addition, we also investigate the effect of candidate sample size in Table 7. We notice that DiffuSeq benefits more from large sample sets (e.g., when the sample size increases from 1 to 10) than RDMs. We attribute this to the possibility that adding Gaussian noise to token embeddings in DiffuSeq might lead to more diverse samples. This helps make better use of the MBR decoding, indicating that there might

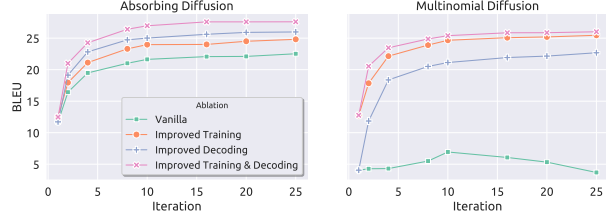


Figure 2: The ablation study of improved training and decoding strategies for both absorbing diffusion (**left**) and multinomial diffusion (**right**) on WMT14 EN-DE test set.

be room to improve RDMs to leverage multiple decodes. Nevertheless, RDMs still achieve better performance than DiffuSeq across both cases of single and multiple samples.

5.3. Analysis

On the Effect of Training and Decoding Strategies. In this section, we investigate the effect of improved training (§4.2) and decoding (§4.3), respectively, as inspired by our reparameterization. In terms of training, our model simplifies the loss objective function of conventional discrete diffusion models to a standard cross-entropy loss, which can be improved further by adopting reweighting strategies. As for decoding, the reparameterized formulation suggests that the uncovered routing mechanism can be made discriminative instead of denoising tokens completely randomly. We ablate the effect of these components and visualize the comparison in Figure 2 (as well as Figures 4a and 4b in Appendix G.2). It can be seen that adopting either the advanced training or decoding scheme would lead to a significant performance boost over vanilla baselines, which can be further enhanced by combining these two improvements together. In particular, we find that the poor performance of vanilla multinomial diffusion stems from *both* insufficient training and ineffective decoding. Either improving the training and decoding would lead to gains of over 10~20 BLEU points, and makes the model scale well to more iteration steps. More detailed ablation studies can be found in Appendix E.

On Decoding Speed. This section visualizes the performance-runtime comparison among different text generation models. All models considered here have roughly the same parameter counts (90~110M), and the speed is measured under the setting of 32 batch size on one NVIDIA GeForce RTX 3090 GPU, averaged by 30 runs. As shown in Figure 3, there is a clear trend that RDMs usually run up to 10 \times faster than a similar-sized auto-regressive baseline GPT2 (Radford et al., 2019), while to achieve similar performance, continuous diffusion models are several orders of magnitude slower than GPT2. Furthermore, discrete diffusion models here are trained with 50 time steps in to-

Table 1: BLEU score comparisons on IWSLT14 DE-EN, WMT14 EN-DE, and WMT16 EN-RO benchmarks. * denotes results reported from previous work.

	Model	# Iterations	IWSLT14 DE-EN		WMT16 EN-RO		WMT14 EN-DE	
			Vanilla	Reparam.	Vanilla	Reparam.	Vanilla	Reparam.
Continuous Diffusion	CDCD (Dieleman et al., 2022)	200	–	–	–	–	20.0*	20.0*
Discrete Diffusion	Multinomial Diffusion (Hoogeboom et al., 2021)	2	23.05	28.01	26.61	30.16	4.28	21.43
		4	24.24	30.57	27.81	31.70	4.31	24.05
		10	21.28	32.23	25.25	33.00	6.94	25.63
		16	20.59	32.58	24.36	33.11	6.07	25.64
		25	20.06	32.84	23.94	33.31	3.69	26.04
	Absorbing Diffusion (Austin et al., 2021)	2	25.24	27.60	27.24	30.72	16.46	21.00
		4	26.93	31.47	29.16	32.60	19.48	24.26
		10	28.32	33.91	30.41	33.38	21.62	26.96
		16	28.38	34.41	30.79	33.82	22.07	27.58
		25	28.93	34.49	30.56	33.99	22.52	27.59
Auto-regressive Models	Transformer-base (Vaswani et al., 2017)	n.a.	34.51		34.16		27.53	

Table 2: Comparisons among different text generators on QG and QQP tasks. Numbers are taken from Gong et al. (2022). [†] denotes results due to our implementation. All discrete diffusion models are run with 10 iterations.

Task	Model	BLEU \uparrow	ROUGE-L \uparrow	BERTScore \uparrow	Dist-1 \uparrow
QG	Transformer-base	0.0364	0.1994	0.5334	0.8236
	GPT2-base FT	0.0741	0.2714	0.6052	0.9602
	GPT2-large FT	0.1110	0.3215	0.6346	0.9670
	GPVAE-T5	0.1251	0.3390	0.6308	0.9381
	NAR-LevT	0.0930	0.2893	0.5491	0.8914
	DiffuSeq	0.1731	0.3665	0.6123	0.9056
	Absorbing [†]	0.1738	0.3503	0.6312	0.9095
	RDM-absorbing [†]	0.1791	0.3565	0.6393	0.9202
	Multinomial [†]	0.1696	0.3429	0.6188	0.8990
	RDM-multinomial [†]	0.1802	0.3550	0.6310	0.9082
QQP	Transformer-base	0.0580	0.2489	0.5392	0.7889
	GPT2-base FT	0.1980	0.5212	0.8246	0.9798
	GPT2-large FT	0.2059	0.5415	0.8363	0.9819
	GPVAE-T5	0.2409	0.5886	0.8466	0.9688
	NAR-LevT	0.2268	0.5795	0.8344	0.9790
	DiffuSeq	0.2413	0.5880	0.8365	0.9807
	Absorbing [†]	0.2382	0.5834	0.8294	0.9566
	RDM-absorbing [†]	0.2510	0.5945	0.8472	0.9849
	Multinomial [†]	0.2070	0.5539	0.7985	0.9175
	RDM-multinomial [†]	0.2498	0.5886	0.8466	0.9817

tal but are able to achieve satisfactory quality even with 2 or 5 steps. In contrast, the continuous diffusion model DiffuSeq, trained with 2000 time steps, mostly generates non-meaningful sentences (BLEU scores getting close to zero) under down-sampled time steps, even equipped with advanced samplers like DDIM (Song et al., 2021a). This reveals the inherent difference between discrete and continuous diffusion, where discrete diffusion generalizes much better to various setups of iteration steps.

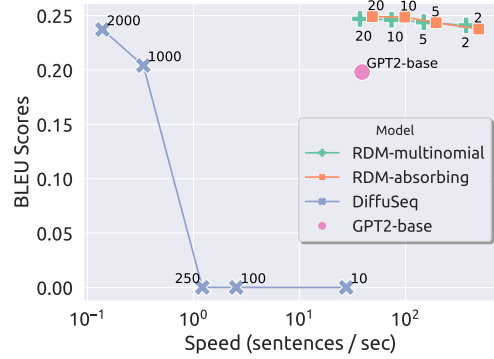


Figure 3: The generation quality-speed comparison among different models for QQP. The annotation indicates the iteration steps except for GPT2, which does not have a fixed number of iterations. The horizontal axis is in log scale.

5.4. Examples

In this section, we conduct a qualitative analysis to showcase the advantages of our model by illustrating the generated samples from the QQP task. We focus on the case of multinomial diffusion and its reparameterized variant; a more comprehensive analysis can be found in Appendix G.3.

Multinomial Diffusion Does Not Decode Iteratively.

As seen in Table 3, vanilla multinomial diffusion only generates the hypothesis at the *first* iteration and gets stuck in the same state thereafter. This means multinomial diffusion decodes in one shot and does not leverage the iterative process for further refinement. In Appendix G.3, we show that this abnormal behavior is primarily due to its degenerated backward formulation, which can be neatly fixed by our reparameterization. The resulting behavior is much more

Table 3: Qualitative samples of test paraphrases generated from different diffusion models on QQP dataset. \ddagger texts are truncated to fit into the table. Words are in lower case.

		Source: how can one increase concentration?
		Reference: how can i improve my concentration?
	# Iter.	Decodes
DiffuSeq	0	o skeptical coli ##zam gael erika calves wharf [unused791] \ddagger
	500	o cessna i perez newark ? venezuelan regeneration 283 zhejiang \ddagger
	1000	o johanna 730 i improve terminals ?
	1500	o how do i improve concentration ?
	2000	o how do i improve concentration ?
	0	o ##tly distances outline ##cera khmer curvature question ##l
Multinomial	1	o how can i improve focus in concentration ?
	2	o how can i improve focus in concentration ?
	3	o how can i improve focus in concentration ?
	4	o how can i improve focus in concentration ?
	5	o how can i improve focus in concentration ?
	0	o lungs ##down intensity cortes ##lden ufo oldies
RDM-multinomial	1	o worker blurred i ##kal caledonia concentration ##vb
	2	o how trait i ##kal my concentration ##vb
	3	o how trait i increase my concentration ?
	3	o how trait i increase my concentration ?
	5	o how do i increase my concentration ?

expected and leads to better generation quality.

The Slow Convergence of Continuous Diffusion. We also demonstrate the down-sampled dynamics during the generation of DiffuSeq. In contrast to discrete diffusion models, where relevant tokens emerge within only a few steps, continuous diffusion hardly decodes meaningful tokens until the 1000-th iteration or later. This validates our hypothesis that the Gaussian diffusion over token embeddings is noisy and slow by design; furthermore, many diffusing steps are required to emit a significant change over token states due to the rounding quantization (see Table 8 for an illustration).

6. Related Work

6.1. Discrete Diffusion Probabilistic Models

Discrete diffusion probabilistic models are first explored in Sohl-Dickstein et al. (2015) for Bernoulli data. Multinomial diffusion (Hoogeboom et al., 2021) later proposes a uniform corruption process for categorical variables, which are extended by D3PMs (Austin et al., 2021) to support general transition matrices, including an absorbing variant that draws close connections to masked language models (Devlin et al., 2019). Several recent works push this line of research further in various aspects, such as incorporating editing-based operations (Johnson et al., 2021; Reid et al., 2022), casting permuted language models (Yang et al., 2019) as diffusion models (Hoogeboom et al., 2022a), developing a continuous-time framework (Campbell et al., 2022), as well as exploring an analog of score functions for learning

the reverse process Sun et al. (2022).

Discrete diffusion has been applied to a variety of tasks, including graph generation (Seff et al., 2019; Haefeli et al., 2022; Vignac et al., 2022), image generation (Esser et al., 2021; Bond-Taylor et al., 2022; Gu et al., 2022; Tang et al., 2022; Hu et al., 2022a), vision-language generation (Hu et al., 2022b), and general multimodal conditional synthesis (Zhu et al., 2022). Lezama et al. (2022) draws connections between discrete diffusion processes and non-autoregressive Transformers for visual domains (Chang et al., 2022; Yu et al., 2022; Chang et al., 2023). For natural language texts, it is initially evaluated on language modeling tasks (Hoogeboom et al., 2021; Austin et al., 2021) despite limited success; recent work adapts discrete diffusion to various text tasks and improves the performance by devising more effective training strategies (Savinov et al., 2022; Qian et al., 2022), designing adaptive noise schedules (He et al., 2022), combining autoregressive decoding as well as edit-based operations (Reid et al., 2022), or incorporating advanced search algorithms (Qian et al., 2022). We refer readers to Cao et al. (2022); Croitoru et al. (2022); Yang et al. (2022) for a detailed review of recent advances in diffusion models.

6.2. Non-autoregressive Text Generation

Diffusion-based generative models also closely relate to iterative non-autoregressive generation (Gu et al., 2018) in the context of machine translation, allowing sequences to be decoded in parallel. The generation process often takes the form of iterative refinement (Lee et al., 2018; Ghazvininejad et al., 2019; Kasai et al., 2020; Ghazvininejad et al., 2020; Huang et al., 2022), which can also be equipped with editing operations (Stern et al., 2019; Gu et al., 2019). Our adaptive routing mechanism (§4.3) closely resembles the heuristic in CMLM (Ghazvininejad et al., 2019), which refines the sequence by masking tokens with low model confidence. Nevertheless, our work proposes a more generic family of discrete diffusion models, which not only justifies the usage of these heuristic decoding algorithms but also implies simple yet effective training methods.

Text Generation with Continuous Diffusion. There has been a surge of interest in adapting continuous diffusion models for text generation. This line of work conducts Gaussian diffusion over the embedding space and achieves appealing results (Li et al., 2022; Gong et al., 2022; Dieleman et al., 2022; Strudel et al., 2022; Lin et al., 2022; Yuan et al., 2022; Gao et al., 2022). Some works consider converting discrete tokens to bit strings and model them as real values (Chen et al., 2022), or injecting Gaussian noise to token logits instead of embeddings (Han et al., 2022). Lovelace et al. (2022) also considers learning a latent continuous diffusion from pre-trained auto-regressive models.

7. Conclusion

This work presents an extensive analysis of discrete diffusion models. Based on the developed understanding, we propose a family of *reparameterized discrete diffusion models* (RDMs) that significantly improve previous work in both training and decoding. We evaluate the proposed diffusion models in various text generation benchmarks and demonstrate the significantly boosted generation quality.

RDMs define a general framework for discrete diffusion processes and can be extended in several ways. For instance, RDMs are currently confined to generating *fixed-length* sentences and rely on an explicit length prediction module to propose the sequence length. It would be interesting to extend the model to enable variable-length sequence generation. Besides, our proposed adaptive routing mechanism (§4.3) makes the initial attempt to unleash the expressiveness of RDMs; the shared training objective (§4.2) allows more advanced search methods to be incorporated into the sampling process for better generation quality. A further investigation into this direction is left as future work.

References

Austin, J., Johnson, D. D., Ho, J., Tarlow, D., and van den Berg, R. Structured denoising diffusion models in discrete state-spaces. In Beygelzimer, A., Dauphin, Y., Liang, P., and Vaughan, J. W. (eds.), *Advances in Neural Information Processing Systems*, 2021. URL <https://openreview.net/forum?id=h7-XixPCAL>.

Balaji, Y., Nah, S., Huang, X., Vahdat, A., Song, J., Kreis, K., Aittala, M., Aila, T., Laine, S., Catanzaro, B., et al. ediffi: Text-to-image diffusion models with an ensemble of expert denoisers. *arXiv preprint arXiv:2211.01324*, 2022.

Bojar, O., Buck, C., Federmann, C., Haddow, B., Koehn, P., Leveling, J., Monz, C., Pecina, P., Post, M., Saint-Amand, H., Sorice, R., Specia, L., and Tamchyna, A. Findings of the 2014 workshop on statistical machine translation. In *Proceedings of the Ninth Workshop on Statistical Machine Translation*, pp. 12–58, Baltimore, Maryland, USA, June 2014. Association for Computational Linguistics. doi: 10.3115/v1/W14-3302. URL <https://aclanthology.org/W14-3302>.

Bojar, O., Chatterjee, R., Federmann, C., Graham, Y., Haddow, B., Huck, M., Jimeno Yepes, A., Koehn, P., Logacheva, V., Monz, C., Negri, M., Névéol, A., Neves, M., Popel, M., Post, M., Rubino, R., Scarton, C., Specia, L., Turchi, M., Verspoor, K., and Zampieri, M. Findings of the 2016 conference on machine translation. In *Proceedings of the First Conference on Machine Translation: Volume 2, Shared Task Papers*, pp. 131–198, Berlin, Germany, August 2016. Association for Computational Linguistics. doi: 10.18653/v1/W16-2301. URL <https://aclanthology.org/W16-2301>.

Bond-Taylor, S., Hessey, P., Sasaki, H., Breckon, T. P., and Willcocks, C. G. Unleashing transformers: parallel token prediction with discrete absorbing diffusion for fast high-resolution image generation from vector-quantized codes. In *European Conference on Computer Vision*, pp. 170–188. Springer, 2022.

Campbell, A., Benton, J., Bortoli, V. D., Rainforth, T., Deligiannidis, G., and Doucet, A. A continuous time framework for discrete denoising models. In Oh, A. H., Agarwal, A., Belgrave, D., and Cho, K. (eds.), *Advances in Neural Information Processing Systems*, 2022. URL <https://openreview.net/forum?id=DmT862YAieY>.

Cao, H., Tan, C., Gao, Z., Chen, G., Heng, P.-A., and Li, S. Z. A survey on generative diffusion model. *arXiv preprint arXiv:2209.02646*, 2022.

Cettolo, M., Niehues, J., Stüker, S., Bentivogli, L., and Federico, M. Report on the 11th IWSLT evaluation campaign. In *Proceedings of the 11th International Workshop on Spoken Language Translation: Evaluation Campaign*, pp. 2–17, Lake Tahoe, California, December 4–5 2014. URL <https://aclanthology.org/2014.iwslt-evaluation.1>.

Chang, H., Zhang, H., Jiang, L., Liu, C., and Freeman, W. T. Maskgit: Masked generative image transformer. In *Proceedings of the IEEE/CVF Conference on Computer Vision and Pattern Recognition*, pp. 11315–11325, 2022.

Chang, H., Zhang, H., Barber, J., Maschinot, A., Lezama, J., Jiang, L., Yang, M.-H., Murphy, K., Freeman, W. T., Rubinstein, M., et al. Muse: Text-to-image generation via masked generative transformers. *arXiv preprint arXiv:2301.00704*, 2023.

Chen, T., Zhang, R., and Hinton, G. Analog bits: Generating discrete data using diffusion models with self-conditioning. *arXiv preprint arXiv:2208.04202*, 2022.

Croitoru, F.-A., Hondu, V., Ionescu, R. T., and Shah, M. Diffusion models in vision: A survey. *arXiv preprint arXiv:2209.04747*, 2022.

Devlin, J., Chang, M.-W., Lee, K., and Toutanova, K. BERT: Pre-training of deep bidirectional transformers for language understanding. In *Proceedings of the 2019 Conference of the North American Chapter of the Association for Computational Linguistics: Human Language Technologies, Volume 1 (Long and Short Papers)*, pp. 4171–4186, Minneapolis, Minnesota, June 2019. Association for

Computational Linguistics. doi: 10.18653/v1/N19-1423.
 URL <https://aclanthology.org/N19-1423>.

Dhingra, B., Mazaitis, K., and Cohen, W. W. Quasar: Datasets for question answering by search and reading. *arXiv preprint arXiv:1707.03904*, 2017.

Dieleman, S., Sartran, L., Roshannai, A., Savinov, N., Ganin, Y., Richemond, P. H., Doucet, A., Strudel, R., Dyer, C., Durkan, C., et al. Continuous diffusion for categorical data. *arXiv preprint arXiv:2211.15089*, 2022.

Esser, P., Rombach, R., Blattmann, A., and Ommer, B. Imagebart: Bidirectional context with multinomial diffusion for autoregressive image synthesis. *Advances in Neural Information Processing Systems*, 34:3518–3532, 2021.

Gao, Z., Guo, J., Tan, X., Zhu, Y., Zhang, F., Bian, J., and Xu, L. Difformer: Empowering diffusion model on embedding space for text generation. *arXiv preprint arXiv:2212.09412*, 2022.

Ghazvininejad, M., Levy, O., Liu, Y., and Zettlemoyer, L. Mask-predict: Parallel decoding of conditional masked language models. In *Proceedings of the 2019 Conference on Empirical Methods in Natural Language Processing and the 9th International Joint Conference on Natural Language Processing (EMNLP-IJCNLP)*, pp. 6112–6121, Hong Kong, China, November 2019. Association for Computational Linguistics. doi: 10.18653/v1/D19-1633. URL <https://aclanthology.org/D19-1633>.

Ghazvininejad, M., Levy, O., and Zettlemoyer, L. Semi-autoregressive training improves mask-predict decoding. *arXiv preprint arXiv:2001.08785*, 2020.

Gong, S., Li, M., Feng, J., Wu, Z., and Kong, L. Diffuseq: Sequence to sequence text generation with diffusion models. *arXiv preprint arXiv:2210.08933*, 2022.

Gu, J., Bradbury, J., Xiong, C., Li, V. O., and Socher, R. Non-autoregressive neural machine translation. In *International Conference on Learning Representations*, 2018. URL <https://openreview.net/forum?id=B118Bt1Cb>.

Gu, J., Wang, C., and Zhao, J. Levenshtein transformer. *Advances in Neural Information Processing Systems*, 32, 2019.

Gu, S., Chen, D., Bao, J., Wen, F., Zhang, B., Chen, D., Yuan, L., and Guo, B. Vector quantized diffusion model for text-to-image synthesis. In *Proceedings of the IEEE/CVF Conference on Computer Vision and Pattern Recognition*, pp. 10696–10706, 2022.

Haefeli, K. K., Martinkus, K., Perraudeau, N., and Wattenhofer, R. Diffusion models for graphs benefit from discrete state spaces. *arXiv preprint arXiv:2210.01549*, 2022.

Han, X., Kumar, S., and Tsvetkov, Y. Ssd-lm: Semi-autoregressive simplex-based diffusion language model for text generation and modular control. *arXiv preprint arXiv:2210.17432*, 2022.

He, Z., Sun, T., Wang, K., Huang, X., and Qiu, X. Diffusionbert: Improving generative masked language models with diffusion models. *arXiv preprint arXiv:2211.15029*, 2022.

Ho, J., Jain, A., and Abbeel, P. Denoising diffusion probabilistic models. In Larochelle, H., Ranzato, M., Hadsell, R., Balcan, M., and Lin, H. (eds.), *Advances in Neural Information Processing Systems*, volume 33, pp. 6840–6851, 2020. URL <https://proceedings.neurips.cc/paper/2020/file/4c5bcfec8584af0d967f1ab10179ca4b-Paper.pdf>.

Ho, J., Salimans, T., Gritsenko, A., Chan, W., Norouzi, M., and Fleet, D. J. Video diffusion models. *arXiv preprint arXiv:2204.03458*, 2022.

Hoogeboom, E., Nielsen, D., Jaini, P., Forré, P., and Welling, M. Argmax flows and multinomial diffusion: Learning categorical distributions. In Beygelzimer, A., Dauphin, Y., Liang, P., and Vaughan, J. W. (eds.), *Advances in Neural Information Processing Systems*, 2021. URL <https://openreview.net/forum?id=6nbPqUCIi7>.

Hoogeboom, E., Gritsenko, A. A., Bastings, J., Poole, B., van den Berg, R., and Salimans, T. Autoregressive diffusion models. In *International Conference on Learning Representations*, 2022a. URL <https://openreview.net/forum?id=Lm8T39vLDTE>.

Hoogeboom, E., Satorras, V. G., Vignac, C., and Welling, M. Equivariant diffusion for molecule generation in 3D. In Chaudhuri, K., Jegelka, S., Song, L., Szepesvari, C., Niu, G., and Sabato, S. (eds.), *Proceedings of the 39th International Conference on Machine Learning*, volume 162 of *Proceedings of Machine Learning Research*, pp. 8867–8887. PMLR, 17–23 Jul 2022b. URL <https://proceedings.mlr.press/v162/hoogeboom22a.html>.

Hu, M., Wang, Y., Cham, T.-J., Yang, J., and Suganthan, P. N. Global context with discrete diffusion in vector quantised modelling for image generation. In *Proceedings of the IEEE/CVF Conference on Computer Vision and Pattern Recognition*, pp. 11502–11511, 2022a.

Hu, M., Zheng, C., Zheng, H., Cham, T.-J., Wang, C., Yang, Z., Tao, D., and Suganthan, P. N. Unified discrete diffusion for simultaneous vision-language generation. *arXiv preprint arXiv:2211.14842*, 2022b.

Huang, X. S., Perez, F., and Volkovs, M. Improving non-autoregressive translation models without distillation. In *International Conference on Learning Representations*, 2022. URL <https://openreview.net/forum?id=I2Hw58KHp80>.

Jo, J., Lee, S., and Hwang, S. J. Score-based generative modeling of graphs via the system of stochastic differential equations. In Chaudhuri, K., Jegelka, S., Song, L., Szepesvari, C., Niu, G., and Sabato, S. (eds.), *Proceedings of the 39th International Conference on Machine Learning*, volume 162 of *Proceedings of Machine Learning Research*, pp. 10362–10383. PMLR, 17–23 Jul 2022. URL <https://proceedings.mlr.press/v162/jo22a.html>.

Johnson, D. D., Austin, J., van den Berg, R., and Tarlow, D. Beyond in-place corruption: Insertion and deletion in denoising probabilistic models. In *ICML Workshop on Invertible Neural Networks, Normalizing Flows, and Explicit Likelihood Models*, 2021. URL <https://openreview.net/forum?id=cAsVBUE1Rnj>.

Karras, T., Aittala, M., Aila, T., and Laine, S. Elucidating the design space of diffusion-based generative models. In Oh, A. H., Agarwal, A., Belgrave, D., and Cho, K. (eds.), *Advances in Neural Information Processing Systems*, 2022. URL <https://openreview.net/forum?id=k7FuTOWM0c7>.

Kasai, J., Cross, J., Ghazvininejad, M., and Gu, J. Non-autoregressive machine translation with disentangled context transformer. In *International conference on machine learning*, pp. 5144–5155. PMLR, 2020.

Kim, Y. and Rush, A. M. Sequence-level knowledge distillation. In *Proceedings of the 2016 Conference on Empirical Methods in Natural Language Processing*, pp. 1317–1327, Austin, Texas, November 2016. Association for Computational Linguistics. doi: 10.18653/v1/D16-1139. URL <https://aclanthology.org/D16-1139>.

Kong, Z., Ping, W., Huang, J., Zhao, K., and Catanzaro, B. Diffwave: A versatile diffusion model for audio synthesis. In *International Conference on Learning Representations*, 2021. URL <https://openreview.net/forum?id=a-xFK8Ymz5J>.

Kool, W., Van Hoof, H., and Welling, M. Stochastic beams and where to find them: The gumbel-top-k trick for sampling sequences without replacement. In *International Conference on Machine Learning*, pp. 3499–3508. PMLR, 2019.

Kool, W., van Hoof, H., and Welling, M. Ancestral gumbel-top-k sampling for sampling without replacement. *Journal of Machine Learning Research*, 21(47):1–36, 2020. URL <http://jmlr.org/papers/v21/19-985.html>.

Lee, J., Mansimov, E., and Cho, K. Deterministic non-autoregressive neural sequence modeling by iterative refinement. In *Proceedings of the 2018 Conference on Empirical Methods in Natural Language Processing*, pp. 1173–1182, Brussels, Belgium, October–November 2018. Association for Computational Linguistics. doi: 10.18653/v1/D18-1149. URL <https://aclanthology.org/D18-1149>.

Lezama, J., Chang, H., Jiang, L., and Essa, I. Improved masked image generation with token-critic. In *European Conference on Computer Vision*, pp. 70–86. Springer, 2022.

Li, X. L., Thickstun, J., Gulrajani, I., Liang, P., and Hashimoto, T. Diffusion-LM improves controllable text generation. In Oh, A. H., Agarwal, A., Belgrave, D., and Cho, K. (eds.), *Advances in Neural Information Processing Systems*, 2022. URL <https://openreview.net/forum?id=3s9IrEsjLyk>.

Lin, Z., Gong, Y., Shen, Y., Wu, T., Fan, Z., Lin, C., Chen, W., and Duan, N. Genie: Large scale pre-training for text generation with diffusion model. *arXiv preprint arXiv:2212.11685*, 2022.

Lovelace, J., Kishore, V., Wan, C., Shekhtman, E., and Weinberger, K. Latent diffusion for language generation. *arXiv preprint arXiv:2212.09462*, 2022.

Nichol, A. Q. and Dhariwal, P. Improved denoising diffusion probabilistic models. In *International Conference on Machine Learning*, pp. 8162–8171. PMLR, 2021.

Ott, M., Edunov, S., Baevski, A., Fan, A., Gross, S., Ng, N., Grangier, D., and Auli, M. fairseq: A fast, extensible toolkit for sequence modeling. In *Proceedings of the 2019 Conference of the North American Chapter of the Association for Computational Linguistics (Demonstrations)*, pp. 48–53, Minneapolis, Minnesota, June 2019. Association for Computational Linguistics. doi: 10.18653/v1/N19-4009. URL <https://aclanthology.org/N19-4009>.

Peebles, W. and Xie, S. Scalable diffusion models with transformers. *arXiv preprint arXiv:2212.09748*, 2022.

Qian, L., Wang, M., Liu, Y., and Zhou, H. Diff-glat: Diffusion glancing transformer for parallel sequence to sequence learning. *arXiv preprint arXiv:2212.10240*, 2022.

Radford, A., Wu, J., Child, R., Luan, D., Amodei, D., Sutskever, I., et al. Language models are unsupervised multitask learners. *OpenAI blog*, 1(8):9, 2019.

Ramesh, A., Dhariwal, P., Nichol, A., Chu, C., and Chen, M. Hierarchical text-conditional image generation with clip latents. *arXiv preprint arXiv:2204.06125*, 2022.

Reid, M., Hellendoorn, V. J., and Neubig, G. Diffuser: Discrete diffusion via edit-based reconstruction. *arXiv preprint arXiv:2210.16886*, 2022.

Richemond, P. H., Dieleman, S., and Doucet, A. Categorical sdes with simplex diffusion. *arXiv preprint arXiv:2210.14784*, 2022.

Rombach, R., Blattmann, A., Lorenz, D., Esser, P., and Ommer, B. High-resolution image synthesis with latent diffusion models. In *Proceedings of the IEEE/CVF Conference on Computer Vision and Pattern Recognition*, pp. 10684–10695, 2022.

Saharia, C., Chan, W., Saxena, S., Li, L., Whang, J., Denton, E., Ghasemipour, S. K. S., Gontijo-Lopes, R., Ayan, B. K., Salimans, T., Ho, J., Fleet, D. J., and Norouzi, M. Photorealistic text-to-image diffusion models with deep language understanding. In Oh, A. H., Agarwal, A., Belgrave, D., and Cho, K. (eds.), *Advances in Neural Information Processing Systems*, 2022. URL <https://openreview.net/forum?id=08Yk-n512A1>.

Savinov, N., Chung, J., Binkowski, M., Elsen, E., and van den Oord, A. Step-unrolled denoising autoencoders for text generation. In *International Conference on Learning Representations*, 2022. URL <https://openreview.net/forum?id=T0GpzBQ1Fg6>.

Seff, A., Zhou, W., Damani, F., Doyle, A., and Adams, R. P. Discrete object generation with reversible inductive construction. *Advances in Neural Information Processing Systems*, 32, 2019.

Sennrich, R., Haddow, B., and Birch, A. Neural machine translation of rare words with subword units. In *Proceedings of the 54th Annual Meeting of the Association for Computational Linguistics (Volume 1: Long Papers)*, pp. 1715–1725, Berlin, Germany, August 2016. Association for Computational Linguistics. doi: 10.18653/v1/P16-1162. URL <https://aclanthology.org/P16-1162>.

Sohl-Dickstein, J., Weiss, E., Maheswaranathan, N., and Ganguli, S. Deep unsupervised learning using nonequilibrium thermodynamics. In *International Conference on Machine Learning*, pp. 2256–2265. PMLR, 2015.

Song, J., Meng, C., and Ermon, S. Denoising diffusion implicit models. In *International Conference on Learning Representations*, 2021a. URL <https://openreview.net/forum?id=St1giarCHLP>.

Song, Y., Sohl-Dickstein, J., Kingma, D. P., Kumar, A., Ermon, S., and Poole, B. Score-based generative modeling through stochastic differential equations. In *International Conference on Learning Representations*, 2021b. URL <https://openreview.net/forum?id=PxTIG12RRHS>.

Stern, M., Chan, W., Kiros, J., and Uszkoreit, J. Insertion transformer: Flexible sequence generation via insertion operations. In *International Conference on Machine Learning*, pp. 5976–5985. PMLR, 2019.

Strudel, R., Tallec, C., Altché, F., Du, Y., Ganin, Y., Mensch, A., Grathwohl, W., Savinov, N., Dieleman, S., Sifre, L., et al. Self-conditioned embedding diffusion for text generation. *arXiv preprint arXiv:2211.04236*, 2022.

Sun, H., Yu, L., Dai, B., Schuurmans, D., and Dai, H. Score-based continuous-time discrete diffusion models. *arXiv preprint arXiv:2211.16750*, 2022.

Tang, Z., Gu, S., Bao, J., Chen, D., and Wen, F. Improved vector quantized diffusion models. *arXiv preprint arXiv:2205.16007*, 2022.

Vahdat, A., Kreis, K., and Kautz, J. Score-based generative modeling in latent space. In Beygelzimer, A., Dauphin, Y., Liang, P., and Vaughan, J. W. (eds.), *Advances in Neural Information Processing Systems*, 2021. URL <https://openreview.net/forum?id=P9TYG0j-wtG>.

Vaswani, A., Shazeer, N., Parmar, N., Uszkoreit, J., Jones, L., Gomez, A. N., Kaiser, Ł., and Polosukhin, I. Attention is all you need. In *Advances in neural information processing systems*, pp. 5998–6008, 2017.

Vieira, T. Gumbel-max trick and weighted reservoir sampling, 2014. URL <http://timvieira.github.io/blog/post/2014/08/01/gumbel-max-trick-and-weighted-reservoir-sampling/>

Vignac, C., Krawczuk, I., Siraudin, A., Wang, B., Cevher, V., and Frossard, P. Digress: Discrete denoising diffusion for graph generation. *arXiv preprint arXiv:2209.14734*, 2022.

Yang, L., Zhang, Z., Song, Y., Hong, S., Xu, R., Zhao, Y., Shao, Y., Zhang, W., Cui, B., and Yang, M.-H. Diffusion models: A comprehensive survey of methods and applications. *arXiv preprint arXiv:2209.00796*, 2022.

Yang, Z., Dai, Z., Yang, Y., Carbonell, J., Salakhutdinov, R. R., and Le, Q. V. Xlnet: Generalized

autoregressive pretraining for language understanding. In Wallach, H., Larochelle, H., Beygelzimer, A., d’Alché-Buc, F., Fox, E., and Garnett, R. (eds.), *Advances in Neural Information Processing Systems*, volume 32, pp. 5753–5763. Curran Associates, Inc., 2019. URL <https://proceedings.neurips.cc/paper/2019/file/dc6a7e655d7e5840e66733e9ee67cc69-Paper.pdf>.

Yu, L., Cheng, Y., Sohn, K., Lezama, J., Zhang, H., Chang, H., Hauptmann, A. G., Yang, M.-H., Hao, Y., Essa, I., et al. Magvit: Masked generative video transformer. *arXiv preprint arXiv:2212.05199*, 2022.

Yuan, H., Yuan, Z., Tan, C., Huang, F., and Huang, S. Seqdiffuseq: Text diffusion with encoder-decoder transformers. *arXiv preprint arXiv:2212.10325*, 2022.

Zhu, Y., Wu, Y., Olszewski, K., Ren, J., Tulyakov, S., and Yan, Y. Discrete contrastive diffusion for cross-modal and conditional generation. *arXiv preprint arXiv:2206.07771*, 2022.

Appendices

A. Extended Background about Discrete Diffusion Models

A.1. The derivation of ELBO

Discrete diffusion models are typically trained by maximizing a lower bound of its marginal log likelihood, defined as below,

$$\begin{aligned}
 & \log p_{\theta}(\mathbf{x}_0) \\
 &= \log \int p_{\theta}(\mathbf{x}_0, \mathbf{x}_1, \dots, \mathbf{x}_T) d\mathbf{x}_1 \cdots d\mathbf{x}_T \\
 &= \log \int \frac{p_{\theta}(\mathbf{x}_0, \mathbf{x}_1, \dots, \mathbf{x}_T)}{q(\mathbf{x}_1, \dots, \mathbf{x}_T | \mathbf{x}_0)} q(\mathbf{x}_1, \dots, \mathbf{x}_T | \mathbf{x}_0) d\mathbf{x}_1 \cdots d\mathbf{x}_T \\
 &= \log \mathbb{E}_{q(\mathbf{x}_1, \dots, \mathbf{x}_T | \mathbf{x}_0)} \left[\frac{p_{\theta}(\mathbf{x}_0, \mathbf{x}_1, \dots, \mathbf{x}_T)}{q(\mathbf{x}_1, \dots, \mathbf{x}_T | \mathbf{x}_0)} \right] \\
 &\geq \mathbb{E}_{q(\mathbf{x}_1, \dots, \mathbf{x}_T | \mathbf{x}_0)} \left[\log \frac{p_{\theta}(\mathbf{x}_0, \mathbf{x}_1, \dots, \mathbf{x}_T)}{q(\mathbf{x}_1, \dots, \mathbf{x}_T | \mathbf{x}_0)} \right] \\
 &= \mathbb{E}_{q(\mathbf{x}_1, \dots, \mathbf{x}_T | \mathbf{x}_0)} \left[\log \frac{p_{\theta}(\mathbf{x}_0 | \mathbf{x}_1) p_{\theta}(\mathbf{x}_T) \prod_{t=2}^T p_{\theta}(\mathbf{x}_{t-1} | \mathbf{x}_t)}{q(\mathbf{x}_T | \mathbf{x}_0) \prod_{t=2}^T q(\mathbf{x}_{t-1} | \mathbf{x}_t, \mathbf{x}_0)} \right] \\
 &= \mathbb{E}_{q(\mathbf{x}_1, \dots, \mathbf{x}_T | \mathbf{x}_0)} \left[\log p_{\theta}(\mathbf{x}_0 | \mathbf{x}_1) - \sum_{t=2}^T \log \frac{q(\mathbf{x}_{t-1} | \mathbf{x}_t, \mathbf{x}_0)}{p_{\theta}(\mathbf{x}_{t-1} | \mathbf{x}_t)} - \log \frac{q(\mathbf{x}_T | \mathbf{x}_0)}{p_{\theta}(\mathbf{x}_T)} \right] \\
 &= \mathbb{E}_q \left[\log p_{\theta}(\mathbf{x}_0 | \mathbf{x}_1) - \sum_{t=2}^T \text{KL}(q(\mathbf{x}_{t-1} | \mathbf{x}_t, \mathbf{x}_0) \| p_{\theta}(\mathbf{x}_{t-1} | \mathbf{x}_t)) - \text{KL}(q(\mathbf{x}_T | \mathbf{x}_0) \| p_{\theta}(\mathbf{x}_T)) \right] \\
 &= \underbrace{\mathbb{E}_{q(\mathbf{x}_1 | \mathbf{x}_0)} [\log p_{\theta}(\mathbf{x}_0 | \mathbf{x}_1)]}_{\mathcal{L}_1(\theta)} - \sum_{t=2}^T \underbrace{\mathbb{E}_{q(\mathbf{x}_t | \mathbf{x}_0)} [\text{KL}(q(\mathbf{x}_{t-1} | \mathbf{x}_t, \mathbf{x}_0) \| p_{\theta}(\mathbf{x}_{t-1} | \mathbf{x}_t))]}_{\mathcal{L}_t(\theta)} + \text{const.} \tag{9}
 \end{aligned}$$

A.2. Parameterization

Recall that our objective is to minimize the KL divergence between $q(\mathbf{x}_{t-1} | \mathbf{x}_t, \mathbf{x}_0)$ and a parameterized distribution $p_{\theta}(\mathbf{x}_{t-1} | \mathbf{x}_t)$ at each time step. A widely adopted way is then defining $p_{\theta}(\mathbf{x}_{t-1} | \mathbf{x}_t) = q(\mathbf{x}_{t-1} | \mathbf{x}_t, \tilde{\mathbf{x}}_0)$, where $\tilde{\mathbf{x}}_0 = f(\mathbf{x}_t; \theta)$ is predicted by a Transformer model. Austin et al. (2021) considers an alternative parameterization by letting $p_{\theta}(\mathbf{x}_{t-1} | \mathbf{x}_t) \propto \sum_{\tilde{\mathbf{x}}_0} q(\mathbf{x}_{t-1}, \mathbf{x}_t | \tilde{\mathbf{x}}_0) p_{\theta}(\tilde{\mathbf{x}}_0 | \mathbf{x}_t)$, where we learn $p_{\theta}(\tilde{\mathbf{x}}_0 | \mathbf{x}_t)$ similarly to $f(\mathbf{x}_t; \theta)$. These two approaches are different in general and define distinct generative processes in general; we follow the former method due to its simplicity and conciseness. More details can be found below.

A.3. Backward Transition Probabilities

This section provides separate derivations for the original backward transition formulation of various discrete diffusion processes.

Absorbing Diffusion. The absorbing diffusion (Austin et al., 2021) defines a Markov chain where a token goes into an absorbing mask state denoted by $[M]$ with some probability at each time step and stays the same thereafter. The forward transition probability is defined as $q(\mathbf{x}_t | \mathbf{x}_{t-1}) = \beta_t \mathbf{x}_{t-1} + (1 - \beta_t) q_{\text{noise}}$, where $q_{\text{noise}} = [M]$ is the point mass with all of the probability on an absorbing state (the mask state $[M]$ is denoted as a one-hot vector).

Regarding the conditional backward transition probability $q(\mathbf{x}_{t-1} | \mathbf{x}_t, \mathbf{x}_0)$, \mathbf{x}_t can only stay in either state \mathbf{x}_0 or state $[M]$. If

$\mathbf{x}_t = \mathbf{x}_0$, then \mathbf{x}_{t-1} must also be in state \mathbf{x}_0 since it is not absorbed yet; while if $\mathbf{x}_t = \mathbf{e}_{[M]}$, we have

$$q(\mathbf{x}_{t-1} = [M] | \mathbf{x}_t = [M], \mathbf{x}_0) = \frac{q(\mathbf{x}_t = [M] | \mathbf{x}_{t-1} = [M])q(\mathbf{x}_{t-1} = [M] | \mathbf{x}_0)}{q(\mathbf{x}_t = [M] | \mathbf{x}_0)} = \frac{1 \cdot (1 - \alpha_{t-1})}{1 - \alpha_t} = \frac{1 - \alpha_{t-1}}{1 - \alpha_t};$$

$$q(\mathbf{x}_{t-1} = \mathbf{x}_0 | \mathbf{x}_t = [M], \mathbf{x}_0) = \frac{q(\mathbf{x}_t = [M] | \mathbf{x}_{t-1} = \mathbf{x}_0)q(\mathbf{x}_{t-1} = \mathbf{x}_0 | \mathbf{x}_0)}{q(\mathbf{x}_t = [M] | \mathbf{x}_0)} = \frac{(1 - \beta_t)\alpha_{t-1}}{1 - \alpha_t} = \frac{\alpha_{t-1} - \alpha_t}{1 - \alpha_t}.$$

The actual generative process is defined as $p_{\theta}(\mathbf{x}_{t-1} | \mathbf{x}_t) \propto \sum_{\tilde{\mathbf{x}}_0} q(\mathbf{x}_{t-1}, \mathbf{x}_t | \tilde{\mathbf{x}}_0) p_{\theta}(\tilde{\mathbf{x}}_0 | \mathbf{x}_t)$, where we predict the probability vector $p_{\theta}(\tilde{\mathbf{x}}_0 | \mathbf{x}_t) := f_{\tilde{\mathbf{x}}_0}(\mathbf{x}_t; \theta)$ from a Transformer. As shown in Austin et al. (2021), this formulation has a simple expression. Suppose $k \neq [M]$ is one of the K possible states. Note that

- if $\mathbf{x}_t = k \neq [M]$, then due to the joint $q(\mathbf{x}_{t-1}, \mathbf{x}_t | \tilde{\mathbf{x}}_0)$ there is only one entry that is non-zero within the sum $q(\mathbf{x}_{t-1} = k, \mathbf{x}_t = k | \tilde{\mathbf{x}}_0 = k) p_{\theta}(\tilde{\mathbf{x}}_0 = k | \mathbf{x}_t)$. As a result, the reverse distribution becomes a point mass over position k ;
- if $\mathbf{x}_t = [M]$, we have

$$p_{\theta}(\mathbf{x}_{t-1} = [M] | \mathbf{x}_t = [M]) \propto \sum_{\tilde{\mathbf{x}}_0} q(\mathbf{x}_t = [M] | \mathbf{x}_{t-1} = [M]) q(\mathbf{x}_{t-1} = [M] | \tilde{\mathbf{x}}_0) p_{\theta}(\tilde{\mathbf{x}}_0 | \mathbf{x}_t)$$

$$= \sum_{\tilde{\mathbf{x}}_0} (1 - \alpha_{t-1}) p_{\theta}(\tilde{\mathbf{x}}_0 | \mathbf{x}_t) = (1 - \alpha_{t-1}) \sum_{\tilde{\mathbf{x}}_0} p_{\theta}(\tilde{\mathbf{x}}_0 | \mathbf{x}_t) = 1 - \alpha_{t-1};$$

$$p_{\theta}(\mathbf{x}_{t-1} = k | \mathbf{x}_t = [M]) \propto \sum_{\tilde{\mathbf{x}}_0} q(\mathbf{x}_t = [M] | \mathbf{x}_{t-1} = k) q(\mathbf{x}_{t-1} = k | \tilde{\mathbf{x}}_0) p_{\theta}(\tilde{\mathbf{x}}_0 | \mathbf{x}_t)$$

$$= q(\mathbf{x}_t = [M] | \mathbf{x}_{t-1} = k) q(\mathbf{x}_{t-1} = k | \tilde{\mathbf{x}}_0 = k) p_{\theta}(\tilde{\mathbf{x}}_0 = k | \mathbf{x}_t)$$

$$= (\alpha_{t-1} - \alpha_t) p_{\theta}(\tilde{\mathbf{x}}_0 = k | \mathbf{x}_t).$$

They can be easily normalized as well,

$$p_{\theta}(\mathbf{x}_{t-1} = [M] | \mathbf{x}_t = [M]) = \frac{1 - \alpha_{t-1}}{1 - \alpha_t}$$

$$p_{\theta}(\mathbf{x}_{t-1} = k | \mathbf{x}_t = [M]) = \frac{(\alpha_{t-1} - \alpha_t) p_{\theta}(\tilde{\mathbf{x}}_0 = k | \mathbf{x}_t)}{1 - \alpha_t}.$$

This can be written in a more compact way, where $p_{\theta}(\tilde{\mathbf{x}}_0 = k | \mathbf{x}_t) := f_k(\mathbf{x}_t; \theta)$ and $q_{\text{noise}} = [M]$ is a point mass with all the probability put over the absorbing state [M].

$$p_{\theta}(\mathbf{x}_{t-1} | \mathbf{x}_t) = \begin{cases} \left(1 - \frac{1 - \alpha_{t-1}}{1 - \alpha_t}\right) f(\mathbf{x}_t; \theta) + \frac{1 - \alpha_{t-1}}{1 - \alpha_t} q_{\text{noise}}, & \text{if } \mathbf{x}_t = [M] \\ \mathbf{x}_t, & \text{if } \mathbf{x}_t \neq [M]. \end{cases} \quad (10)$$

We can also generalize this result for $0 < s < t \leq T$. For the forward transition, we have $q(\mathbf{x}_t | \mathbf{x}_s = \mathbf{x}_0) = \prod_{i=s+1}^t \beta_i \mathbf{x}_0 + \left(1 - \prod_{i=s+1}^t \beta_i\right) q_{\text{noise}} = \frac{\alpha_t}{\alpha_s} \mathbf{x}_0 + \frac{\alpha_s - \alpha_t}{\alpha_s} q_{\text{noise}}$. Thus the backward transition can be derived as well according to Bayes' rule,

$$q(\mathbf{x}_s | \mathbf{x}_t, \mathbf{x}_0) = \begin{cases} \frac{\alpha_s - \alpha_t}{1 - \alpha_t} \mathbf{x}_0 + \frac{1 - \alpha_s}{1 - \alpha_t} q_{\text{noise}}, & \text{if } \mathbf{x}_t = [M] \\ \mathbf{x}_t, & \text{if } \mathbf{x}_t \neq [M]. \end{cases} \quad (11)$$

$$p_{\theta}(\mathbf{x}_s | \mathbf{x}_t) = \begin{cases} \frac{\alpha_s - \alpha_t}{1 - \alpha_t} f(\mathbf{x}_t; \theta) + \frac{1 - \alpha_s}{1 - \alpha_t} q_{\text{noise}}, & \text{if } \mathbf{x}_t = [M] \\ \mathbf{x}_t, & \text{if } \mathbf{x}_t \neq [M]. \end{cases} \quad (12)$$

Multinomial Diffusion. In multinomial diffusion (Hoogeboom et al., 2021), the forward transition probability is defined as $q(\mathbf{x}_t|\mathbf{x}_{t-1}) = \beta_t \mathbf{x}_{t-1} + (1 - \beta_t)q_{\text{noise}}$, where $q_{\text{noise}} = \mathbf{1}/K$ is a uniform distribution over $\{1, 2, \dots, K\}$ with $\mathbf{1}$ is a K -dimensional vector with all ones. The backward transition probability conditional on the original data \mathbf{x}_0 can be derived according to Bayes' rule and in closed form:

$$\begin{aligned} q(\mathbf{x}_{t-1}|\mathbf{x}_t, \mathbf{x}_0) &= \frac{q(\mathbf{x}_t|\mathbf{x}_{t-1})q(\mathbf{x}_{t-1}|\mathbf{x}_0)}{q(\mathbf{x}_t|\mathbf{x}_0)} \\ &= \frac{(\beta_t \mathbf{x}_t + (1 - \beta_t) \frac{\mathbf{1}}{K}) \odot (\alpha_{t-1} \mathbf{x}_0 + (1 - \alpha_{t-1}) \frac{\mathbf{1}}{K})}{\mathbf{x}_t^\top (\alpha_t \mathbf{x}_0 + (1 - \alpha_t) \frac{\mathbf{1}}{K})} \\ &= \frac{\alpha_t \mathbf{x}_t \odot \mathbf{x}_0 + \frac{1}{K} \beta_t (1 - \alpha_{t-1}) \mathbf{x}_t + \frac{1}{K} (1 - \beta_t) \alpha_{t-1} \mathbf{x}_0 + \frac{1}{K^2} (1 - \beta_t) (1 - \alpha_{t-1}) \mathbf{1}}{\alpha_t \mathbf{x}_t^\top \mathbf{x}_0 + \frac{1}{K} (1 - \alpha_t)}. \end{aligned} \quad (13)$$

Multinomial diffusion (Hoogeboom et al., 2021) learns a parameterized distribution $p_{\theta}(\mathbf{x}_{t-1}|\mathbf{x}_t)$ to approximate $q(\mathbf{x}_{t-1}|\mathbf{x}_t, \mathbf{x}_0)$ at each time step, which is defined as $p_{\theta}(\mathbf{x}_{t-1}|\mathbf{x}_t) = q(\mathbf{x}_{t-1}|\mathbf{x}_t, \tilde{\mathbf{x}}_0)$ with $\tilde{\mathbf{x}}_0 = f(\mathbf{x}_t; \theta)$ being the output by a Transformer model.

$$p_{\theta}(\mathbf{x}_{t-1}|\mathbf{x}_t) = \frac{\alpha_t \mathbf{x}_t \odot f(\mathbf{x}_t; \theta) + \frac{1}{K} \beta_t (1 - \alpha_{t-1}) \mathbf{x}_t + \frac{1}{K} (1 - \beta_t) \alpha_{t-1} f(\mathbf{x}_t; \theta) + \frac{1}{K^2} (1 - \beta_t) (1 - \alpha_{t-1}) \mathbf{1}}{\alpha_t \mathbf{x}_t^\top f(\mathbf{x}_t; \theta) + \frac{1}{K} (1 - \alpha_t)}. \quad (14)$$

B. Derivation for Proposition 3.1

In this section, we provide the derivation for Equation 2 based on Bayes' rule.

Proof. We denote $\mathbf{P}_t \in \mathbb{R}^{K \times K}$ as the probability transition matrix for the t -th step, where $[\mathbf{P}_t]_{ij} = p(\mathbf{x}_t = j|\mathbf{x}_{t-1} = i)$ and thus the probability distribution in the forward process can be described as $q(\mathbf{x}_t|\mathbf{x}_{t-1}) = \text{Categorical}(\mathbf{x}_t; \mathbf{P}_t^\top \mathbf{x}_{t-1})$. It is then easy to see that

$$q(\mathbf{x}_t|\mathbf{x}_0) = \sum_{\mathbf{x}_{t-1}, \mathbf{x}_{t-2}, \dots, \mathbf{x}_1} q(\mathbf{x}_t, \mathbf{x}_{t-1}, \mathbf{x}_{t-2}, \dots, \mathbf{x}_1|\mathbf{x}_0) = \text{Categorical}(\mathbf{x}_t; \bar{\mathbf{P}}_t^\top \mathbf{x}_0)$$

with $\bar{\mathbf{P}}_t = \mathbf{P}_1 \mathbf{P}_2 \dots \mathbf{P}_t$. Returning to our case where the forward transition takes the form $q(\mathbf{x}_t|\mathbf{x}_{t-1}) = \beta_t \mathbf{x}_{t-1} + (1 - \beta_t)q_{\text{noise}}$. The transition matrix can be represented by $\mathbf{P}_t = \beta_t \mathbf{I} + (1 - \beta_t) \mathbf{1} q_{\text{noise}}^\top$, and thus $\bar{\mathbf{P}}_t = \mathbf{P}_1 \mathbf{P}_2 \dots \mathbf{P}_t = \alpha_t \mathbf{I} + (1 - \alpha_t) \mathbf{1} q_{\text{noise}}^\top$. Equipped with these results, we can proceed with the derivation as follows,

$$\begin{aligned} q(\mathbf{x}_{t-1}|\mathbf{x}_t, \mathbf{x}_0) &= \frac{q(\mathbf{x}_t|\mathbf{x}_{t-1})q(\mathbf{x}_{t-1}|\mathbf{x}_0)}{q(\mathbf{x}_t|\mathbf{x}_0)} = \frac{\mathbf{P}_t \mathbf{x}_t \odot \bar{\mathbf{P}}_{t-1}^\top \mathbf{x}_0}{\mathbf{x}_t^\top \bar{\mathbf{P}}_t^\top \mathbf{x}_0} \\ &= \frac{[\beta_t \mathbf{x}_t + (1 - \beta_t) \sigma_{\mathbf{x}_t} \mathbf{1}] \odot [\alpha_{t-1} \mathbf{x}_0 + (1 - \alpha_{t-1}) q_{\text{noise}}]}{\alpha_t \mathbf{x}_t^\top \mathbf{x}_0 + (1 - \alpha_t) \mathbf{x}_t^\top q_{\text{noise}}} \\ &= \frac{\beta_t \alpha_{t-1} \mathbf{x}_t \odot \mathbf{x}_0 + \beta_t (1 - \alpha_{t-1}) \mathbf{x}_t \odot q_{\text{noise}} + (1 - \beta_t) \alpha_{t-1} \sigma_{\mathbf{x}_t} \mathbf{1} \odot \mathbf{x}_0 + (1 - \beta_t) (1 - \alpha_{t-1}) \sigma_{\mathbf{x}_t} \mathbf{1} \odot q_{\text{noise}}}{\alpha_t \mathbf{x}_t^\top \mathbf{x}_0 + (1 - \alpha_t) \mathbf{x}_t^\top q_{\text{noise}}} \\ &= \frac{\beta_t \alpha_{t-1} \mathbf{x}_t \odot \mathbf{x}_0 + \beta_t (1 - \alpha_{t-1}) \sigma_{\mathbf{x}_t} \mathbf{x}_t + (1 - \beta_t) \alpha_{t-1} \sigma_{\mathbf{x}_t} \mathbf{x}_0 + (1 - \beta_t) (1 - \alpha_{t-1}) \sigma_{\mathbf{x}_t} q_{\text{noise}}}{\alpha_t \mathbf{x}_t^\top \mathbf{x}_0 + (1 - \alpha_t) \sigma_{\mathbf{x}_t}}. \end{aligned}$$

Here we denote \odot as element-wise product and $\sigma_{\mathbf{x}_t} := q_{\text{noise}}(\mathbf{u} = \mathbf{x}_t)$ to represent the probability of noise drawn from q_{noise} being equal to \mathbf{x}_t . The need to differentiate between \mathbf{x}_t and \mathbf{x}_0 emerges when we calculate $\mathbf{x}_t \odot \mathbf{x}_0$, which would be an all-zero vector $\mathbf{0}$ except that it would be one if $\mathbf{x}_t = \mathbf{x}_0$. Thus the computation of backward transition probabilities breaks down into two cases:

- If $\mathbf{x}_t = \mathbf{x}_0$, we have $\mathbf{x}_t \odot \mathbf{x}_0 = \mathbf{x}_t, \mathbf{x}_t^\top \mathbf{x}_0 = 1$ and thus

$$\begin{aligned} q(\mathbf{x}_{t-1}|\mathbf{x}_t, \mathbf{x}_0) &= \frac{\beta_t \alpha_{t-1} \mathbf{x}_t + \beta_t (1 - \alpha_{t-1}) \sigma_{\mathbf{x}_t} \mathbf{x}_t + (1 - \beta_t) \alpha_{t-1} \sigma_{\mathbf{x}_t} \mathbf{x}_t + (1 - \beta_t) (1 - \alpha_{t-1}) \sigma_{\mathbf{x}_t} q_{\text{noise}}}{\alpha_t + (1 - \alpha_t) \sigma_{\mathbf{x}_t}} \\ &= \frac{\beta_t \alpha_{t-1} + \beta_t (1 - \alpha_{t-1}) \sigma_{\mathbf{x}_t} + (1 - \beta_t) \alpha_{t-1} \sigma_{\mathbf{x}_t} \mathbf{x}_t + (1 - \beta_t) (1 - \alpha_{t-1}) \sigma_{\mathbf{x}_t} q_{\text{noise}}}{\alpha_t + (1 - \alpha_t) \sigma_{\mathbf{x}_t}}. \end{aligned}$$

- If $\mathbf{x}_t \neq \mathbf{x}_0$, we have $\mathbf{x}_t \odot \mathbf{x}_0 = \mathbf{0}$, $\mathbf{x}_t \top \mathbf{x}_0 = 0$ and thus

$$\begin{aligned}
 q(\mathbf{x}_{t-1} | \mathbf{x}_t, \mathbf{x}_0) &= \frac{\beta_t(1 - \alpha_{t-1})\sigma_{\mathbf{x}_t} \mathbf{x}_t + (1 - \beta_t)\alpha_{t-1}\sigma_{\mathbf{x}_t} \mathbf{x}_0 + (1 - \beta_t)(1 - \alpha_{t-1})\sigma_{\mathbf{x}_t} q_{\text{noise}}}{(1 - \alpha_t)\sigma_{\mathbf{x}_t}} \\
 &= \frac{\beta_t(1 - \alpha_{t-1})\mathbf{x}_t + (1 - \beta_t)\alpha_{t-1}\mathbf{x}_0 + (1 - \beta_t)(1 - \alpha_{t-1})q_{\text{noise}}}{1 - \alpha_t} \\
 &= \frac{(1 - \beta_t)\alpha_{t-1}}{1 - \alpha_t}\mathbf{x}_0 + \frac{\beta_t(1 - \alpha_{t-1})}{1 - \alpha_t}\mathbf{x}_t + \frac{(1 - \beta_t)(1 - \alpha_{t-1})}{1 - \alpha_t}q_{\text{noise}} \\
 &= \frac{(1 - \beta_t)\alpha_{t-1}}{1 - \alpha_t}\mathbf{x}_0 + \frac{1 - \alpha_{t-1}}{1 - \alpha_t}[\beta_t\mathbf{x}_t + (1 - \beta_t)q_{\text{noise}}] \\
 &= \frac{\alpha_{t-1} - \alpha_t}{1 - \alpha_t}\mathbf{x}_0 + \left(1 - \frac{\alpha_{t-1} - \alpha_t}{1 - \alpha_t}\right)[\beta_t\mathbf{x}_t + (1 - \beta_t)q_{\text{noise}}].
 \end{aligned}$$

Putting them together, we arrive at the resulting formulation,

$$q(\mathbf{x}_{t-1} | \mathbf{x}_t, \mathbf{x}_0) = \begin{cases} \lambda_{t-1}^{(1)}\mathbf{x}_t + \left(1 - \lambda_{t-1}^{(1)}\right)q_{\text{noise}}, & \text{if } \mathbf{x}_t = \mathbf{x}_0 \\ \lambda_{t-1}^{(2)}\mathbf{x}_0 + \left(1 - \lambda_{t-1}^{(2)}\right)q_{\text{noise}}(\mathbf{x}_t), & \text{if } \mathbf{x}_t \neq \mathbf{x}_0. \end{cases}$$

Here $\lambda_{t-1}^{(1)} := 1 - \frac{(1 - \beta_t)(1 - \alpha_{t-1})q_{\text{noise}}(\mathbf{u} = \mathbf{x}_t)}{\alpha_t + (1 - \alpha_t)q_{\text{noise}}(\mathbf{u} = \mathbf{x}_t)}$, $\lambda_{t-1}^{(2)} := \frac{\alpha_{t-1} - \alpha_t}{1 - \alpha_t}$, and $q_{\text{noise}}(\mathbf{x}_t) = \beta_t\mathbf{x}_t + (1 - \beta_t)q_{\text{noise}}$ denotes a noise distribution that interpolates between \mathbf{x}_t and q_{noise} , both of which are possibly noisy.

Generalization. Similar to vanilla diffusion models, we can also derive backward transition processes with a gap Δ_t ; that is, we consider $q(\mathbf{x}_s | \mathbf{x}_t, \mathbf{x}_0)$ with $s = t - \Delta_t$. It can be easily seen that

$$q(\mathbf{x}_s | \mathbf{x}_t, \mathbf{x}_0) = \begin{cases} \lambda_s^{(1)}\mathbf{x}_t + \left(1 - \lambda_s^{(1)}\right)q_{\text{noise}}, & \text{if } \mathbf{x}_t = \mathbf{x}_0 \\ \lambda_s^{(2)}\mathbf{x}_0 + \left(1 - \lambda_s^{(2)}\right)q_{\text{noise}}(\mathbf{x}_t), & \text{if } \mathbf{x}_t \neq \mathbf{x}_0, \end{cases} \quad (15)$$

with $\lambda_s^{(1)} := 1 - \frac{(1 - \alpha_s)(1 - \alpha_s)q_{\text{noise}}(\mathbf{u} = \mathbf{x}_t)}{\alpha_t + (1 - \alpha_t)q_{\text{noise}}(\mathbf{u} = \mathbf{x}_t)}$ and $\lambda_s^{(2)} := \frac{\alpha_s - \alpha_t}{1 - \alpha_t}$. \square

C. Derivations for the ELBO of RDMs

The following provides the derivation for the loss objective of RDMs.

$$\begin{aligned}
 \log p(\mathbf{x}_0) &\geq \mathbb{E}_{q(\mathbf{x}_{1:T}, \mathbf{v}_{1:T} | \mathbf{x}_0)} \left[\log \frac{p_{\theta}(\mathbf{x}_0, \mathbf{x}_{1:T}, \mathbf{v}_{1:T})}{q(\mathbf{x}_{1:T}, \mathbf{v}_{1:T} | \mathbf{x}_0)} \right] \\
 &= \mathbb{E}_{q(\mathbf{x}_{1:T}, \mathbf{v}_{1:T} | \mathbf{x}_0)} \left[\log \frac{p_{\theta}(\mathbf{x}_0 | \mathbf{x}_1) \prod_{t=2}^T p_{\theta}(\mathbf{x}_{t-1}, \mathbf{v}_{t-1} | \mathbf{x}_t) p(\mathbf{x}_T, \mathbf{v}_T)}{\prod_{t=2}^T q(\mathbf{x}_{t-1}, \mathbf{v}_{t-1} | \mathbf{x}_t, \mathbf{x}_0) q(\mathbf{x}_T, \mathbf{v}_T | \mathbf{x}_0)} \right] \\
 &= \mathbb{E}_{q(\mathbf{x}_{1:T}, \mathbf{v}_{1:T} | \mathbf{x}_0)} \left[\log p_{\theta}(\mathbf{x}_0 | \mathbf{x}_1) + \sum_{t=2}^T \log \frac{p_{\theta}(\mathbf{x}_{t-1}, \mathbf{v}_{t-1} | \mathbf{x}_t)}{q(\mathbf{x}_{t-1}, \mathbf{v}_{t-1} | \mathbf{x}_t, \mathbf{x}_0)} + \log \frac{p(\mathbf{x}_T, \mathbf{v}_T)}{q(\mathbf{x}_T, \mathbf{v}_T | \mathbf{x}_0)} \right] \\
 &= \mathbb{E}_{q(\mathbf{x}_1 | \mathbf{x}_0)} [\log p_{\theta}(\mathbf{x}_0 | \mathbf{x}_1)] - \sum_{t=2}^T \mathbb{E}_{q(\mathbf{x}_t | \mathbf{x}_0)} [\text{KL}(q(\mathbf{x}_{t-1}, \mathbf{v}_{t-1} | \mathbf{x}_t, \mathbf{x}_0) \parallel p_{\theta}(\mathbf{x}_{t-1}, \mathbf{v}_{t-1} | \mathbf{x}_t))] + \text{const.} \\
 &:= \mathcal{L}_1(\theta) - \sum_{t=2}^T \mathcal{L}_t(\theta) + \text{const.}
 \end{aligned}$$

For $t > 1$, we can push the decomposition further,

$$\begin{aligned}
 \mathcal{L}_t(\boldsymbol{\theta}) &= \mathbb{E}_{q(\mathbf{x}_t|\mathbf{x}_0)} [\text{KL}(q(\mathbf{x}_{t-1}, \mathbf{v}_{t-1}|\mathbf{x}_t, \mathbf{x}_0) \parallel p_{\boldsymbol{\theta}}(\mathbf{x}_{t-1}, \mathbf{v}_{t-1}|\mathbf{x}_t))] \\
 &= \mathbb{E}_{q(\mathbf{x}_t|\mathbf{x}_0)} \left[\sum_{\mathbf{x}_{t-1}, \mathbf{v}_{t-1}} q(\mathbf{x}_{t-1}, \mathbf{v}_{t-1}|\mathbf{x}_t, \mathbf{x}_0) \log \frac{q(\mathbf{x}_{t-1}, \mathbf{v}_{t-1}|\mathbf{x}_t, \mathbf{x}_0)}{p_{\boldsymbol{\theta}}(\mathbf{x}_{t-1}, \mathbf{v}_{t-1}|\mathbf{x}_t)} \right] \\
 &= \mathbb{E}_{q(\mathbf{x}_t|\mathbf{x}_0)} \left[\sum_{\mathbf{x}_{t-1}, \mathbf{v}_{t-1}} q(\mathbf{x}_{t-1}|\mathbf{v}_{t-1}, \mathbf{x}_t, \mathbf{x}_0) q(\mathbf{v}_{t-1}) \left[\log \frac{q(\mathbf{x}_{t-1}|\mathbf{v}_{t-1}, \mathbf{x}_t, \mathbf{x}_0)}{p_{\boldsymbol{\theta}}(\mathbf{x}_{t-1}|\mathbf{v}_{t-1}, \mathbf{x}_t)} + \log \frac{q(\mathbf{v}_{t-1})}{p_{\boldsymbol{\theta}}(\mathbf{v}_{t-1})} \right] \right] \\
 &= \mathbb{E}_{q(\mathbf{x}_t|\mathbf{x}_0)} [\mathbb{E}_{q(\mathbf{v}_{t-1})} [\text{KL}(q(\mathbf{x}_{t-1}|\mathbf{v}_{t-1}, \mathbf{x}_t, \mathbf{x}_0) \parallel p_{\boldsymbol{\theta}}(\mathbf{x}_{t-1}|\mathbf{v}_{t-1}, \mathbf{x}_t))] + \text{KL}(q(\mathbf{v}_{t-1}) \parallel p_{\boldsymbol{\theta}}(\mathbf{v}_{t-1}))].
 \end{aligned}$$

D. Derivation for Proposition 4.1

Proof. We first consider the loss objective at each step for *each token* at n -th position, which can be expanded as follows,

$$\mathcal{L}_t^n(\boldsymbol{\theta}) = \mathbb{E}_{q(\mathbf{x}_{t,n}|\mathbf{x}_{0,n})} [\mathbb{E}_{q(\mathbf{v}_{t-1,n})} [\text{KL}(q(\mathbf{x}_{t-1,n}|\mathbf{v}_{t-1,n}, \mathbf{x}_{t,n}, \mathbf{x}_{0,n}) \parallel p_{\boldsymbol{\theta}}(\mathbf{x}_{t-1,n}|\mathbf{v}_{t-1,n}, \mathbf{x}_{t,n}))]].$$

Typically we draw a Monte Carlo sample $\mathbf{x}_{t,n} \sim q(\mathbf{x}_{t,n}|\mathbf{x}_{0,n})$ to estimate the outermost expectation above. For the inner term, recall that $b_{t,n} = \mathbf{1}_{\mathbf{x}_{t,n}=\mathbf{x}_{0,n}}$ and $q(\mathbf{x}_{t-1,n}|\mathbf{v}_{t-1,n}, \mathbf{x}_{t,n}, \mathbf{x}_{0,n})$ takes the form as

$$q(\mathbf{x}_{t-1,n}|\mathbf{v}_{t-1,n}, \mathbf{x}_{t,n}, \mathbf{x}_{0,n}) = \begin{cases} v_{t-1,n}^{(1)} \mathbf{x}_{t,n} + (1 - v_{t-1,n}^{(1)}) q_{\text{noise}}, & \text{if } b_{t,n} = 1 \\ v_{t-1,n}^{(2)} \mathbf{x}_{0,n} + (1 - v_{t-1,n}^{(2)}) q_{\text{noise}}(\mathbf{x}_{t,n}), & \text{if } b_{t,n} = 0. \end{cases}$$

Since we use the teacher-forcing approach that employs the same oracle $b_{t,n}$ for $p_{\boldsymbol{\theta}}(\mathbf{x}_{t-1,n}|\mathbf{v}_{t-1,n}, \mathbf{x}_{t,n})$ as well, it can also be written in a similar manner,

$$p_{\boldsymbol{\theta}}(\mathbf{x}_{t-1,n}|\mathbf{v}_{t-1,n}, \mathbf{x}_{t,n}) = \begin{cases} v_{t-1,n}^{(1)} \mathbf{x}_{t,n} + (1 - v_{t-1,n}^{(1)}) q_{\text{noise}}, & \text{if } b_{t,n} = 1 \\ v_{t-1,n}^{(2)} f(\mathbf{x}_{t,n}; \boldsymbol{\theta}) + (1 - v_{t-1,n}^{(2)}) q_{\text{noise}}(\mathbf{x}_{t,n}), & \text{if } b_{t,n} = 0. \end{cases}$$

The derivation then breaks down into two cases with respect to $b_{t,n}$:

If $b_{t,n} = 1$. In this case, $q(\mathbf{x}_{t-1,n}|\mathbf{v}_{t-1,n}, \mathbf{x}_{t,n}, \mathbf{x}_{0,n}) = p_{\boldsymbol{\theta}}(\mathbf{x}_{t-1,n}|\mathbf{v}_{t-1,n}, \mathbf{x}_{t,n}) = v_{t-1,n}^{(1)} \mathbf{x}_{t,n} + (1 - v_{t-1,n}^{(1)}) q_{\text{noise}}$. Since these two distributions become identical, this leads to zero KL divergence irrespective of $\mathbf{v}_{t-1,n}$ so that $\mathcal{L}_t(\boldsymbol{\theta}) = 0$;

If $b_{t,n} = 0$. In this scenario, we have $q(\mathbf{x}_{t-1,n}|b_{t-1}, \mathbf{x}_{t,n}, \mathbf{x}_{0,n}) = v_{t-1,n}^{(2)} \mathbf{x}_{0,n} + (1 - v_{t-1,n}^{(2)}) q_{\text{noise}}(\mathbf{x}_{t,n})$ and $v_{t-1,n}^{(2)} f(\mathbf{x}_{t,n}; \boldsymbol{\theta}) + (1 - v_{t-1,n}^{(2)}) q_{\text{noise}}(\mathbf{x}_{t,n})$. We then enumerate all the possible outcomes for $v_{t-1,n}^{(2)}$. If $v_{t-1,n}^{(2)} = 1$, $q(\mathbf{v}_{t-1,n}) = \lambda_{t-1}^{(2)}$ and

$$\text{KL}(q(\mathbf{x}_{t-1,n}|\mathbf{v}_{t-1,n}, \mathbf{x}_{t,n}, \mathbf{x}_{0,n}) \parallel p_{\boldsymbol{\theta}}(\mathbf{x}_{t-1,n}|\mathbf{v}_{t-1,n}, \mathbf{x}_{t,n})) = \text{KL}(\mathbf{x}_{0,n} \parallel f(\mathbf{x}_{t,n}; \boldsymbol{\theta})) = -\mathbf{x}_{0,n}^\top \log f(\mathbf{x}_{t,n}; \boldsymbol{\theta}).$$

If $v_{t-1,n}^{(2)} = 0$, then $q(\mathbf{v}_{t-1,n}) = 1 - \lambda_{t-1}^{(2)}$ and

$$\text{KL}(q(\mathbf{x}_{t-1,n}|\mathbf{v}_{t-1,n}, \mathbf{x}_{t,n}, \mathbf{x}_{0,n}) \parallel p_{\boldsymbol{\theta}}(\mathbf{x}_{t-1,n}|\mathbf{v}_{t-1,n}, \mathbf{x}_{t,n})) = \text{KL}(q_{\text{noise}}(\mathbf{x}_{t,n}) \parallel q_{\text{noise}}(\mathbf{x}_{t,n})) = 0.$$

Putting them together, we have

$$\begin{aligned}
 \mathbb{E}_{q(\mathbf{v}_{t-1,n})} [\text{KL}(q(\mathbf{x}_{t-1,n}|\mathbf{v}_{t-1,n}, \mathbf{x}_{t,n}, \mathbf{x}_{0,n}) \parallel p_{\boldsymbol{\theta}}(\mathbf{x}_{t-1,n}|\mathbf{v}_{t-1,n}, \mathbf{x}_{t,n}))] &= -\lambda_{t-1}^{(2)} \mathbf{x}_{0,n}^\top \log f(\mathbf{x}_{t,n}; \boldsymbol{\theta}) + (1 - \lambda_{t-1}^{(2)}) \cdot 0 \\
 &= -\lambda_{t-1}^{(2)} \mathbf{x}_{0,n}^\top \log f(\mathbf{x}_{t,n}; \boldsymbol{\theta}).
 \end{aligned}$$

Since each token is modeled conditionally independently, we can add all computed losses for each token, arriving at the final expression for the whole sequence,

$$\mathcal{L}_t(\boldsymbol{\theta}) = \sum_{n=1}^N \mathcal{L}_t^n(\boldsymbol{\theta}) = \mathbb{E}_{p_{\text{data}}(\mathbf{x}_{0,1:N}) \prod_{n=1}^N q(\mathbf{x}_{t,n}|\mathbf{x}_{0,n})} \left[-\lambda_{t-1}^{(2)} \sum_{n=1}^N (1 - b_{t,n}) \mathbf{x}_{0,n}^\top \log f(\mathbf{x}_{t,n}; \boldsymbol{\theta}) \right].$$

□

E. Additional Implementation Details

This section describes the implementation details of our experiments.

E.1. Tasks

- For all translation tasks, we do *not* adopt knowledge distillation (Kim & Rush, 2016; Gu et al., 2018) that replaces the target side of training data with outputs generated by a pre-trained autoregressive Transformer.
- For both *QG* and *QQP* tasks, we use the same WordPiece tokenization as in BERT (Devlin et al., 2019) and obtain a vocabulary of size 30522.

E.2. Architectures

- We employ the Transformer-base architecture (Vaswani et al., 2017) for WMT experiments, while for *IWSLT14 DE-EN, QG*, and *QQP* tasks we use a smaller Transformer model. Note that all self-attention blocks with the model are bi-directional and do not use causal masks.
- We adopt a length prediction module (Ghazvininejad et al., 2019) on top of the Transformer encoder to propose target length candidates for the generated sequence. Given the source input, we first run the Transformer encoder to obtain the encoder’s hidden representation, which is averaged and passed to a linear layer to output the length scores.
- The timestep embedding is obtained by first projecting the input timestep t with sinusoidal encodings and then passing it through a two-layer MLP.
- We adopt *concatenated* instead of additive position encodings, which is shown to enhance the positional information and produce better performance in the context of machine translation (Huang et al., 2022).

The detailed configuration for the neural network is listed in Table 6.

E.3. Training

- We allocate a large number of diffusion time steps for training, such as 50 or 100. We found the number of diffusion steps *in training* does not affect the performance too much. Note that decoding can be performed with an arbitrary number of iterations by choosing the appropriate step size $\Delta t > 1$. That is, we can decode by sampling $\mathbf{x}_{t-\Delta t} \sim p_{\theta}(\mathbf{x}_{t-\Delta t} | \mathbf{x}_t)$, following a similar treatment as Equation 15.
- As described in §4.2, we can tune the weight $\lambda_{t-1}^{(2)}$ to reweigh the loss objective. We ablate this choice in Table 5 and demonstrate that $\lambda_{t-1}^{(2)} = 1 - \frac{t-1}{T}$, which is a heuristic proposed in (Bond-Taylor et al., 2022), produces the best translation performance on *IWSLT14 DE-EN* dataset. Therefore, we adopt this reweighting scheme by default unless specified otherwise.
- Modern Transformer models usually process input sequences that are associated with some special symbols, such as the begin-of-sentence symbol *<bos>*, eos-of-sentence symbol *<eos>*, padding symbol *<pad>*, and so on. We found it beneficial to treat these special symbols as normal tokens in vanilla/reparameterized absorbing diffusion (and thus these symbols can be noised), but this treatment leads to much worse performance in vanilla/reparameterized multinomial diffusion.
- We also adopt conditioned training (details in Appendix F) to further improve the model, which leads to consistent improvements upon vanilla training. Its effect is ablated in Table 4. In particular, conditioned training leads to almost 2 BLEU improvements over vanilla diffusion processes but the gain becomes marginal for our reparameterized variants.

The detailed configuration for the optimization hyper-parameters is listed in Table 6.

E.4. Decoding

- Note that we train a neural network $f(\cdot; \theta)$ to approximate \mathbf{x}_0 , which is a softmax-normalized probability vector. There are several ways to decode a token from the probability vector, such as simply taking its argmax position or performing sampling with temperatures τ . Empirically, we find a low temperature $\tau = 0.1$, or simply the argmax works well across tasks, and use the argmax approach by default; Nevertheless, the diversity of generated sentences can be improved by adopting a larger temperature as well.

Table 4: BLEU scores on IWSLT14 DE-EN test set with/without conditioned training. The results are evaluated under different diffusion models with 10 decoding iterations. Default decoding strategies are adopted for these models: vanilla multinomial or absorbing diffusion uses vanilla decoding, while reparameterized discrete diffusion models adopt improved decoding.

Conditioned training	Absorbing	Multinomial	RDM-absorbing	RDM-multinomial
\times	28.32	21.28	33.73	31.99
\checkmark	29.67	23.58	33.91	32.23

Table 5: BLEU scores on IWSLT14 DE-EN test set with different reweighting schemes for training. The results are evaluated under RDM-absorbing with 10 decoding iterations.

Reweighting training scheme	Vanilla decoding	Improved decoding
Original $(\lambda_{t-1}^{(2)} = \frac{\alpha_{t-1} - \alpha_t}{1 - \alpha_t})$	28.32	30.64
Linear $(\lambda_{t-1}^{(2)} = 1 - \frac{t-1}{T})$	31.04	33.91
Constant $(\lambda_{t-1}^{(2)} = 1)$	29.75	32.57

- Like common diffusion models, we use an exponential moving average (EMA) to track the model parameters with a decay rate of 0.9999. We also average model parameters among the five last checkpoints for generation, following standard practices in machine translation (Vaswani et al., 2017).
- For translation experiments, we use 5 length candidates, decode them in parallel, and select the sequence with the highest model score as the final output. For question generation and paraphrasing, we follow DiffuSeq (Gong et al., 2022) to use MBR decoding with 10 samples to ensure a head-to-head comparison. The candidates in MBR decoding are generated in the following manner: first selecting 3 length candidates, and then sampling 3,3, and 4 additional sentences for each length size, resulting in 10 candidates in total.
- We also investigate several components of the adaptive decoding algorithm (§4.3) and provide more implementation details below:
 - The top- k selection mechanism in Equation 7, which is deterministic by design, can also be made stochastic. In particular, instead of directly selecting those tokens with top- k largest scores, we first add Gumbel noise to the score $s_{t,n}$ of each token, and then fetch the top- k tokens with the largest perturbed scores. This is inspired by previous work that aims to sample multiple items from a set without replacement (Vieira, 2014; Kool et al., 2019; 2020); however, this simple approach brings several benefits in that the selection of k tokens from the sequence could involve extra randomness, and this might be helpful for exploration during decoding.
 - Recall that during decoding, the role of $\mathbf{v}_{t-1,n}^{(1)}$ is to indicate whether the token can remain in the denoised state, while $\mathbf{v}_{t-1,n}^{(2)}$ is used to denoise the token that is currently noisy. In Equation 7, both of them would be set to 1 as long as the n -th token belongs to the top- k set. However, we observe that $\mathbf{v}_{t-1,n}^{(1)}$ and $\mathbf{v}_{t-1,n}^{(2)}$ can also be generated differently. For example, one might adopt a more conservative approach, where already denoised tokens rarely or never turn back to the noise. We implemented a strategy to achieve this by imposing more constraints over $\mathbf{v}_{t-1,n}^{(1)}$: $\mathbf{v}_{t-1,n}^{(i)} = \mathbf{1}_{(n \in \mathcal{P}_{t-1}) \vee (s_{t,n} > s_{t+1,n}) \vee (\mathbf{x}_{t,n} \neq \mathbf{x}_{t+1,n})}$, where we set $\mathbf{v}_{t-1,n}^{(1)} = 0$ only when its corresponding token score is not in the top- k set and indeed becomes smaller than the previous iteration. Intuitively, this means the denoised tokens should remain as denoised most time, except that the Transformer model becomes less confident and requires re-prediction. This is one of many possible approaches to achieving such control, as our framework allows us to do such conditioning flexibly; we find this strategy works sometimes better than the vanilla approach, especially on IWSLT14 DE-EN dataset.
 - Another important hyper-parameter during decoding is k , the number of tokens to be in denoised states at each iteration for our discriminative routing mechanism (§4.3). To ensure that the degree of noise decreases as the generation process proceeds, we schedule k to increase from 1 to N monotonically as the diffusion step t goes from T to 1. We set k to follow either a {cosine, linear} scheme based on the development set performance. The cosine strategy yields $k = \lfloor \cos \frac{\pi t}{2T} \cdot N \rfloor$, while the linear variant gives $k = \lfloor (1 - \frac{t}{T}) \cdot N \rfloor$.

Table 6: The hyper-parameter configuration for machine translation.

Hyper-parameter	WMT14 EN-DE	WMT16 EN-RO	IWSLT14 DE-EN	QG	QQP
Number of transformer encoder layers	6	6	6	6	6
Number of transformer decoder layers	6	6	6	6	6
Hidden size	512	512	512	512	512
hidden size in FFN	2048	2048	1024	1024	1024
Number of attention heads	8	8	4	8	8
Maximum number of tokens in a batch	128K	32K	4K	—	—
Maximum number of sentences in a batch	—	—	—	256	256
Number of training steps	300K	120K	300K	70K	70K
Number of warm-up steps	10K	15K	30K	10K	10K
Weight decay rate	0.01	0.01	0.01	0.01	0.01
Peak Learning Rate	0.0005	0.0005	0.0005	0.0005	0.0005
Label Smoothing	0.1	0.1	0.1	0.1	0.1
Learning rate decay	Inverse square root				
Optimizer	Adam	Adam	Adam	Adam	Adam
Dropout	0.1	0.3	0.3	0.2	0.2
Gradient Clipping Norm	—	—	—	1.0	1.0

- To perform conditional generation, we delegate the full task of conditioning to the encoder-decoder architecture. That is, instead of designing complicated guidance to condition the diffusion probabilistic process, we treat the conditioning information as the input of the Transformer encoder. This simple strategy is found to work well in practice.

F. Extension: Improved Training with Conditioning

Training discrete diffusion models usually involves a heavy amount of randomness. For instance, at each training iteration, one has to sample a time step and corrupt a random subset of sequence tokens for denoising. To control the introduced variance, we adopt a simple yet effective conditioning strategy that uses multiple samples to perform training. The key idea is conceptually simple: we start with sampling two *i.i.d.* time steps $s, t \sim \text{Uniform}(T)$ (without the loss of generality, we assume $s < t$). After that, we draw $\mathbf{x}_t \sim q(\mathbf{x}_t | \mathbf{x}_0)$ as usual, but condition the sample at step s by drawing from $q(\mathbf{x}_s | \mathbf{x}_0) = \mathbb{E}_{q(\mathbf{x}_t | \mathbf{x}_0)} [q(\mathbf{x}_s | \mathbf{x}_t, \mathbf{x}_0)] \approx q(\mathbf{x}_s | \mathbf{x}_t, \mathbf{x}_0)$. The losses (Equation 6) at step s and t are then estimated individually and averaged to obtain the final training objective. In case $s = t$, we simply drop the conditioning and sample $\mathbf{x}_s \sim q(\mathbf{x}_s | \mathbf{x}_0)$ instead.

This method utilizes multiple samples to estimate the loss objective while remaining unbiased. To see this, note that

$$\begin{aligned}
 & -(\mathcal{L}_s + \mathcal{L}_t) \\
 &= \mathbb{E}_q \left[\log \frac{q(\mathbf{x}_{s-1} | \mathbf{x}_s, \mathbf{x}_0)}{p_{\theta}(\mathbf{x}_{s-1} | \mathbf{x}_s)} + \log \frac{q(\mathbf{x}_{t-1} | \mathbf{x}_t, \mathbf{x}_0)}{p_{\theta}(\mathbf{x}_{t-1} | \mathbf{x}_t)} \right] \\
 &= \mathbb{E}_{q(\mathbf{x}_{s-1}, \mathbf{x}_s, \mathbf{x}_{t-1}, \mathbf{x}_t | \mathbf{x}_0)} \left[\log \frac{q(\mathbf{x}_{s-1} | \mathbf{x}_s, \mathbf{x}_0)}{p_{\theta}(\mathbf{x}_{s-1} | \mathbf{x}_s)} + \log \frac{q(\mathbf{x}_{t-1} | \mathbf{x}_t, \mathbf{x}_0)}{p_{\theta}(\mathbf{x}_{t-1} | \mathbf{x}_t)} \right] \\
 &= \mathbb{E}_{q(\mathbf{x}_{s-1}, \mathbf{x}_s, \mathbf{x}_{t-1}, \mathbf{x}_t | \mathbf{x}_0)} \left[\log \frac{q(\mathbf{x}_{s-1} | \mathbf{x}_s, \mathbf{x}_0)}{p_{\theta}(\mathbf{x}_{s-1} | \mathbf{x}_s)} \right] + \mathbb{E}_{q(\mathbf{x}_{s-1}, \mathbf{x}_s, \mathbf{x}_{t-1}, \mathbf{x}_t | \mathbf{x}_0)} \left[\log \frac{q(\mathbf{x}_{t-1} | \mathbf{x}_t, \mathbf{x}_0)}{p_{\theta}(\mathbf{x}_{t-1} | \mathbf{x}_t)} \right] \\
 &= \mathbb{E}_{q(\mathbf{x}_{s-1}, \mathbf{x}_s, \mathbf{x}_{t-1}, \mathbf{x}_t | \mathbf{x}_0)} \left[\log \frac{q(\mathbf{x}_{s-1} | \mathbf{x}_s, \mathbf{x}_0)}{p_{\theta}(\mathbf{x}_{s-1} | \mathbf{x}_s)} \right] + \mathbb{E}_{q(\mathbf{x}_{t-1}, \mathbf{x}_t | \mathbf{x}_0)} \left[\log \frac{q(\mathbf{x}_{t-1} | \mathbf{x}_t, \mathbf{x}_0)}{p_{\theta}(\mathbf{x}_{t-1} | \mathbf{x}_t)} \right] \\
 &= \mathbb{E}_{q(\mathbf{x}_t | \mathbf{x}_0)q(\mathbf{x}_s | \mathbf{x}_t, \mathbf{x}_0)} [\text{KL}(q(\mathbf{x}_{s-1} | \mathbf{x}_s, \mathbf{x}_0) \parallel p_{\theta}(\mathbf{x}_{s-1} | \mathbf{x}_s))] + \mathbb{E}_{q(\mathbf{x}_t | \mathbf{x}_0)} [\text{KL}(q(\mathbf{x}_{t-1} | \mathbf{x}_t, \mathbf{x}_0) \parallel p_{\theta}(\mathbf{x}_{t-1} | \mathbf{x}_t))].
 \end{aligned}$$

This conditioned training brings several benefits. On the one hand, it introduces explicit coupling between \mathbf{x}_s and \mathbf{x}_t , which can be seen as an application of Rao-blackwellization and constrains the degree of randomness while still maintaining unbiasedness; on the other hand, as we deal with samples from the simulated backward transition $q(\mathbf{x}_s | \mathbf{x}_t, \mathbf{x}_0)$ instead of $q(\mathbf{x}_s | \mathbf{x}_0)$, this formulation aligns better with the generation process. In practice, this technique can be applied to most existing diffusion processes, only amounts to double the batch size within a single model forward pass, and consistently brings large empirical improvements over vanilla discrete diffusion baselines (Table 4). However, the gains become marginal when switched to our reparameterized variants. We hypothesize that this is due to insufficient training in vanilla discrete diffusion models, which is already alleviated in our improved training scheme.

Algorithm 3 Training RDMs with Conditioning

Input: neural network $f(\cdot; \theta)$, data distribution $p_{\text{data}}(\mathbf{x}_{0,1:N})$, and a specified reweighting scalar $\lambda_{t-1}, \lambda_{s-1}$.
Output: model parameters θ .

repeat

 Draw $\mathbf{x}_{0,1:N} \sim p_{\text{data}}(\mathbf{x}_{0,1:N})$;
 Draw $s \in \text{Uniform}(\{1, \dots, T\})$;
 Draw $t \in \text{Uniform}(\{1, \dots, T\})$;
 Swap t and s if necessary so that $s \leq t$;

for $n = 1, 2, \dots, N$ **do**

 Draw $\mathbf{x}_{t,n} \sim q(\mathbf{x}_{t,n} | \mathbf{x}_{0,n})$;
 Let $b_{t,n} = \mathbf{1}_{\mathbf{x}_{t,n} = \mathbf{x}_{0,n}}$;
 if $s = t$ **then**
 Draw $\mathbf{x}_{s,n} \sim q(\mathbf{x}_{s,n} | \mathbf{x}_{0,n})$;
 else
 Draw $\mathbf{x}_{s,n} \sim q(\mathbf{x}_{s,n} | \mathbf{x}_{t,n}, \mathbf{x}_{0,n})$;
 end if
 Let $b_{s,n} = \mathbf{1}_{\mathbf{x}_{s,n} = \mathbf{x}_{0,n}}$;

end for

$\mathcal{L}_t(\theta) = -\lambda_{t-1} \sum_{n=1}^N (1 - b_{t,n}) \mathbf{x}_{0,n}^\top \log f(\mathbf{x}_{t,n}; \theta)$;
 $\mathcal{L}_s(\theta) = -\lambda_{s-1} \sum_{n=1}^N (1 - b_{s,n}) \mathbf{x}_{0,n}^\top \log f(\mathbf{x}_{s,n}; \theta)$;
 Compute $\mathcal{L}(\theta) = \frac{1}{2} (\mathcal{L}_s(\theta) + \mathcal{L}_t(\theta))$;
 Minimize $\mathcal{L}(\theta)$ with respect to θ ;

until converged

G. Additional Experimental Results

G.1. Additional Experiments For Question and Paraphrase Generation

Table 7 presents the comparison between text diffusion models under the different number of candidate samples. We notice that DiffuSeq benefits slightly more from large sample sets (e.g., when the sample size m increases from 1 to 10) than RDMs. We attribute this to the possibility that adding Gaussian noise to token embeddings in DiffuSeq might lead to more diverse samples. This helps make better use of the MBR decoding, indicating that there might be room to improve RDMs to leverage multiple decodes. Nevertheless, RDMs still achieve better performance than DiffuSeq across both cases of single and multiple samples. Note that due to the limited computation resources, our reproduction of DiffuSeq (Gong et al., 2022) adopts a smaller Transformer model with around 36M parameters (aligning with our setting) and runs with a smaller batch size of 256, thus resulting in slightly worse results than those reported.

G.2. Additional Ablation Study For Translation Tasks

This section presents additional plots (Figure 4) that visualize the effect of different components in our model.

G.3. Extended Qualitative Analysis

This section provides a more comprehensive qualitative analysis of different diffusion models, including several generated samples as in Tables 8 to 10.

Multinomial Diffusion Does Not Decode Iteratively. As presented in Tables 8 to 10, multinomial diffusion finishes the generation of most sentences in the first iteration and remains unchanged afterward, despite multiple iteration steps being allocated.

This unexpected behavior is due to the formulation of its original backward process, which is of the form as Equation 14

Table 7: Comparisons among different text generators on QG and QQP tasks. Numbers are taken from Gong et al. (2022). \dagger denotes results due to our implementation. m denotes the number of samples used for MBR decoding. RDM variants are run with 10 iterations.

Task	Model	BLEU \uparrow	ROUGE-L \uparrow	BERTScore \uparrow	Dist-1 \uparrow
QG	Transformer-base	0.0364	0.1994	0.5334	0.8236
	GPT2-base FT	0.0741	0.2714	0.6052	0.9602
	GPT2-large FT	0.1110	0.3215	0.6346	0.9670
	GPVAE-T5	0.1251	0.3390	0.6308	0.9381
	NAR-LevT	0.0930	0.2893	0.5491	0.8914
	DiffuSeq	0.1731	0.3665	0.6123	0.9056
	DiffuSeq † ($m=1$)	0.1405	0.3343	0.5783	0.9109
	RDM-absorbing † ($m=1$)	0.1699	0.3517	0.6286	0.9098
	RDM-multinomial † ($m=1$)	0.1768	0.3559	0.6305	0.9081
QQP	DiffuSeq † ($m=10$)	0.1569	0.3561	0.5945	0.9062
	RDM-absorbing † ($m=10$)	0.1791	0.3565	0.6393	0.9202
	RDM-multinomial † ($m=10$)	0.1802	0.3550	0.6310	0.9082
	Transformer-base	0.0580	0.2489	0.5392	0.7889
	GPT2-base FT	0.1980	0.5212	0.8246	0.9798
	GPT2-large FT	0.2059	0.5415	0.8363	0.9819
	GPVAE-T5	0.2409	0.5886	0.8466	0.9688
	NAR-LevT	0.2268	0.5795	0.8344	0.9790
	DiffuSeq	0.2413	0.5880	0.8365	0.9807
	DiffuSeq † ($m=1$)	0.1845	0.5284	0.7936	0.9739
	RDM-absorbing † ($m=1$)	0.2336	0.5789	0.8374	0.9805
	RDM-multinomial † ($m=1$)	0.2291	0.5725	0.8366	0.9802
	DiffuSeq † ($m=10$)	0.2371	0.5835	0.8327	0.9818
	RDM-absorbing † ($m=10$)	0.2510	0.5945	0.8472	0.9849
	RDM-multinomial † ($m=10$)	0.2498	0.5886	0.8466	0.9817

(copied here for convenience),

$$p_{\theta}(\mathbf{x}_{t-1}|\mathbf{x}_t) = \frac{\alpha_t \mathbf{x}_t \odot f(\mathbf{x}_t; \theta) + \frac{1}{K} \beta_t (1 - \alpha_{t-1}) \mathbf{x}_t + \frac{1}{K} (1 - \beta_t) \alpha_{t-1} f(\mathbf{x}_t; \theta) + \frac{1}{K^2} (1 - \beta_t) (1 - \alpha_{t-1}) \mathbf{1}}{\alpha_t \mathbf{x}_t^\top f(\mathbf{x}_t; \theta) + \frac{1}{K} (1 - \alpha_t)}.$$

Note that $f(\cdot; \theta)$ is a softmax probability vector output from a Transformer model. At the initial iteration, α_t is very close to zero, and the Transformer prediction $f(\cdot; \theta)$ has the chance to come into play and denoise to a certain degree. But when the process moves onward, α_t becomes larger, which will soon make the first term dominate significantly over the others since all the other terms are scaled down by $1/K$. Since the vocabulary size K is usually large in text generation tasks (usually larger than 10K), this would make all the other terms very close to zero. In this case, the backward transition distribution degenerates to

$$p_{\theta}(\mathbf{x}_{t-1}|\mathbf{x}_t) \approx \frac{\alpha_t \mathbf{x}_t \odot f(\mathbf{x}_t; \theta)}{\alpha_t \mathbf{x}_t^\top f(\mathbf{x}_t; \theta)} = \mathbf{x}_t.$$

That is, what multinomial diffusion does after the initial steps is merely copying previous states, and hence the sequence mostly remains unchanged. The only chance for the multinomial diffusion processes to decode is at the initial stage; after then, the model would get stuck in the current state and cannot escape away. This explains why multinomial diffusion does not behave like typical iterative processes.

Our *reparameterization* does not suffer from these issues. Thanks to Equation 2, the developed reparameterized formulation alleviates the need to normalize all terms together; instead, it divides different terms into two cases, which are then normalized separately. This avoids the possibility that different terms are affected by their relative scales. The resulting behavior is much more expected and leads to better generation quality.

The Slow Convergence of Continuous Diffusion. In contrast to discrete diffusion models that can perform generation in 10 steps or fewer, continuous diffusion usually requires thousands of steps to decode a decent sample. We hypothesize that

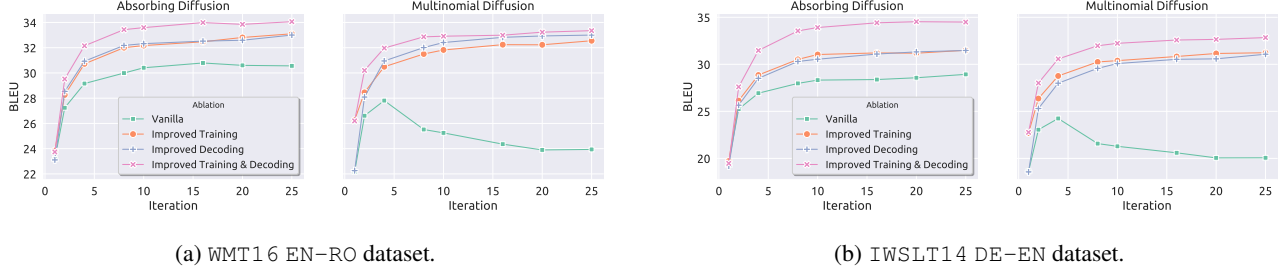


Figure 4: The ablation study of improved training and decoding strategies for both absorbing diffusion and multinomial diffusion on WMT16 EN-RO and IWSLT14 DE-EN test sets.

this is due to two reasons: (1) the noisy and slow Gaussian diffusion over token embeddings by design; (2) furthermore, many diffusing steps are required to emit a significant change over token states due to the rounding operation. We provide empirical evidence for our hypothesis by zooming in to inspect the generation process. As can be seen in Tables 8 and 9, many consecutive steps in continuous diffusion (1000~1009 iteration) do not modify the decode at all, even when it is not converged yet, leading to a potential waste of computation.

Absorbing Diffusion Cannot Fix Previous Errors. While vanilla absorbing diffusion performs decoding more steadily, it also suffers from some issues. As shown in Tables 8 to 10, since all tokens are predicted independently conditional on the source input, there is some chance for the model to decode multiple identical tokens simultaneously. However, in vanilla absorbing diffusion, such decoding errors cannot be fixed. To see this, note that its backward transition formulation can be written as Equation 10, which is copied here for convenience,

$$p_{\theta}(\mathbf{x}_{t-1}|\mathbf{x}_t) = \begin{cases} \left(1 - \frac{1-\alpha_{t-1}}{1-\alpha_t}\right) f(\mathbf{x}_t; \theta) + \frac{1-\alpha_{t-1}}{1-\alpha_t} q_{\text{noise}}, & \text{if } \mathbf{x}_t = [M] \\ \mathbf{x}_t, & \text{if } \mathbf{x}_t \neq [M]. \end{cases}$$

Under this backward formulation, once a token is decoded, it will stay in the state thereafter and does not have the chance to be re-predicted again. As a result, vanilla absorbing diffusion processes cannot fix previously made errors.

This issue can be alleviated by RDMs, which employ a more generic formulation as follows,

$$p_{\theta}(\mathbf{x}_{t-1}|\mathbf{v}_{t-1}, \mathbf{x}_t) = \begin{cases} v_{t-1}^{(1)} \mathbf{x}_t + \left(1 - v_{t-1}^{(1)}\right) q_{\text{noise}}, & \text{if } b_t = 1 \\ v_{t-1}^{(2)} f(\mathbf{x}_t; \theta) + \left(1 - v_{t-1}^{(2)}\right) q_{\text{noise}}(\mathbf{x}_t), & \text{if } b_t = 0. \end{cases}$$

Here b_t is a binary variable indicating whether \mathbf{x}_t is denoised or not, and $v_{t-1}^{(1)}$ can be either 1 or 0, depending on the strategy (§4.3). Therefore, in RDMs, we can allow decoded tokens to be rolled back to noisy states by setting $v_{t-1}^{(1)} = 0$ (e.g., these repetitive tokens might receive lower model scores than the others, which can be recognized as low-confidence outputs in Equation 7). An example can be found in Table 8, where the decoded repetitive tokens `months` at 3-th iteration are then re-masked at the next iteration.

Table 8: A snapshot of all iterations for qualitative samples of test paraphrases generated from different diffusion models on QQP dataset. \ddagger texts are truncated to fit into the table. Words are in lower case. $\langle M \rangle$ stands for mask states, and $\#\#$ denotes the sub-word tokenization artifacts.

Source: i have only 2 months for my ca cpt exams how do i prepare?

Reference: i want to crack ca cpt in 2 months. how should i study?

# Iter.	Decodes
Absorbing	o <M>
	o <M> <M> <M> <M> <M> ca <M> ca <M> <M> ca <M> <M> <M> <M>
	o <M> <M> <M> <M> <M> ca <M> ca <M> <M> ca <M> <M> <M>
	o <M> <M> <M> <M> <M> ca - ca cp <M> ca <M> <M> exam <M>
	o <M> can <M> prepare <M> ca - ca cp <M> ca <M> <M> $\#\#$ t exam ?
	o how can i prepare for ca - ca cp $\#\#$ t ca cp $\#\#$ t exam ?
RDM-absorbing	o <M>
	o how <M> i <M> ?
	o how <M> i prepare for ca <M> $\#\#$ t <M> <M> <M> <M> <M> ?
	o how <M> i prepare for ca cp $\#\#$ t <M> <M> <M> months months ?
	o how <M> i prepare for ca cp $\#\#$ t exam in two months <M> ?
	o how can i prepare for ca cp $\#\#$ t exam in two months left ?
Multinomial	o glossy [unused448] raymond manga subjective questioning suriname masonic listen explored
	o how can i prepare for ca cp $\#\#$ t months ?
	o how can i prepare for ca cp $\#\#$ t months ?
	o how can i prepare for ca cp $\#\#$ t months ?
	o how can i prepare for ca cp $\#\#$ t months ?
	o how can i prepare for ca cp $\#\#$ t months ?
RDM-multinomial	o consonants $\#\#$ nin leading elegance 406 173 militant teams $\#\#$ nin dyke thee seafood
	o how residues i $\#\#$ fighting sentences malaysian jenkins remembers transatlantic universite $\#\#$ rp monarch ?
	o how can i cyril for malaysian jenkins goldberg transatlantic in relationships pursuing ?
	o how can i chu for ca fashionable $\#\#$ t exam in clerks months ?
	o how can i prepare for ca cp $\#\#$ t exam in 2 months ?
	o how can i prepare for ca cp $\#\#$ t exam in 2 months ?
DiffuSeq	o defective thereby evaluation michaels fragments primal electrically aground hostilities \ddagger
	o simulcast candidacy $\#\#$ bner [unused106] $\#\#$ wide subgenus dangerously sincerity resolving migrated menon $\#\#$ lase \ddagger
	o westphalia $\#\#$ tracted universite $\#\#$ erly reissued neglect showcased [unused574] slade \ddagger
	o souza electronically compliant gerard priority townships $\#\#$ neo hidalgo [unused574] \ddagger
	o spikes peptide $\#\#$ ales borneo makeshift moi rebelled neglect textual 1899 erasmus publishes \ddagger
	o i reduces griffin $\#\#$ ales bukit makeshift moi $\#\#$ slaw mcbride how ministries \ddagger
	o i [unused582] to gazing monterrey makeshift ca wastewater norton , how ministries can \ddagger
	o i [unused582] to gazing monterrey makeshift ca iata norton , how ministries can \ddagger
	o i [unused582] to gazing monterrey makeshift ca iata norton , how ministries can \ddagger
	o i [unused582] to gazing monterrey makeshift ca iata norton , how ministries can \ddagger
1250	o i [unused582] to gazing monterrey makeshift ca iata norton , how ministries can \ddagger
	o i [unused582] to gazing monterrey makeshift ca iata norton , how ministries can \ddagger
	o i [unused582] to gazing monterrey makeshift ca iata norton , how ministries can \ddagger
	o i [unused582] to gazing monterrey makeshift ca iata norton , how ministries can \ddagger
	o i [unused582] to gazing monterrey makeshift ca iata norton , how ministries can \ddagger
	o i [unused582] to gazing monterrey makeshift ca iata norton , how ministries can \ddagger
1500	o i want to prepare $\#\#$ cchi my ca glove henan rouen how synthesized can [unused201] $\#\#$ yya exam ?
	o i want to prepare for my ca cp exam , how transvaal can warmed $\#\#$ yya exam ?
	o i want to prepare for my ca cp exam , how yun can get 2 exam ?
	o i want to prepare for my ca cp exam , how might can get 2 exam ?

Table 9: A snapshot of all iterations for qualitative samples of test paraphrases generated from different diffusion models on QQP dataset. \ddagger texts are truncated to fit into the table. Words are in lower case. $\langle M \rangle$ stands for mask states, and $\#\#$ denotes the sub-word tokenization artifacts.

		Source: how can one increase concentration?	Reference: how can i improve my concentration?
		Decodes	
# Iter.			
Absorbing	0	o $\langle M \rangle \langle M \rangle$	
	1	o $\langle M \rangle$ can i increase $\langle M \rangle \langle M \rangle \langle M \rangle \langle M \rangle$	
	2	o how can i increase concentration $\langle M \rangle \langle M \rangle \langle M \rangle$	
	3	o how can i increase concentration in studying $\langle M \rangle$	
	4	o how can i increase concentration in studying $\langle M \rangle$	
	5	o how can i increase concentration in studying ?	
RDM-absorbing	0	o $\langle M \rangle \langle M \rangle$	
	1	o $\langle M \rangle \langle M \rangle \langle M \rangle \langle M \rangle \langle M \rangle$ concentration ?	
	2	o how $\langle M \rangle \langle M \rangle \langle M \rangle$ my concentration ?	
	3	o how $\langle M \rangle \langle M \rangle$ increase my concentration ?	
	4	o how $\langle M \rangle$ i increase my concentration ?	
	5	o how can i increase my concentration ?	
Multinomial	0	o $\#\#$ tly distances outline $\#\#$ cera khmer curvature question $\#\#$ tl	
	1	o how can i improve focus in concentration ?	
	2	o how can i improve focus in concentration ?	
	3	o how can i improve focus in concentration ?	
	4	o how can i improve focus in concentration ?	
	5	o how can i improve focus in concentration ?	
RDM-multinomial	0	o lungs $\#\#$ down intensity cortes $\#\#$ lden ufo oldies	
	1	o worker blurted i $\#\#$ kal caledonia concentration $\#\#$ vb	
	2	o how trait i $\#\#$ kal my concentration $\#\#$ vb	
	3	o how trait i increase my concentration ?	
	4	o how trait i increase my concentration ?	
	5	o how do i increase my concentration ?	
DiffuSeq	0	o skeptical coli $\#\#$ zam gael erika calves wharf [unused791] $\#\#$ pta vhf $\#\#$ kley adoptive \ddagger	
	10	o encompassing hesse informally campos cosmopolitan postmaster stabilization realised \ddagger	
	100	o thump haitian i $\#\#$ anov xiv ? $\#\#$ norris illuminated $\#\#$ had kilometers disagreed [unused730] \ddagger	
	250	o fatal correlated trenton i $\#\#$ anov exhibits $\#\#$ scandinavia 1934 plaza leveled 910 \ddagger	
	500	o cessna i perez newark ? venezuelan regeneration 283 zhejiang $\#\#$ hectares [PAD] \ddagger	
	750	o johanna cessna i perez shriek ? [PAD] [PAD] [PAD] [PAD] rahman [PAD] [PAD] [PAD] postmaster \ddagger	
	1000	o johanna 730 i improve terminals ?	
	1001	o johanna 730 i improve terminals ?	
	1002	o johanna 730 i improve terminals ?	
	1003	o johanna 730 i improve terminals ?	
	1004	o johanna 730 i improve terminals ?	
	1005	o johanna 730 i improve terminals ?	
	1006	o johanna 730 i improve terminals ?	
	1007	o johanna 730 i improve terminals ?	
	1008	o johanna 730 i improve terminals ?	
	1009	o johanna 730 i improve terminals ?	
	1250	o how do i improve concentration ?	
	1500	o how do i improve concentration ?	
	1750	o how do i improve concentration ?	
	2000	o how do i improve concentration ?	

Table 10: A snapshot of all iterations for generated translates from different diffusion models on IWSLT14 DE-EN benchmark. Words are in lower case. <M> stands for mask states, and ## denotes the sub-word tokenization artifacts.

Source: alleine dieser flughafen hat eine fläche von 100 quadratkilometern .

Reference: this airport alone covers more than 100 square kilometers .

# Iter.		Decodes
Absorbing	0	o <M>
	1	o <M> <M> <M> <M> <M> has an an <M> of <M> <M> miles <M>
	2	o <M> <M> <M> <M> <M> has an an <M> of <M> <M> miles <M>
	3	o <M> <M> air## <M> <M> has an an <M> of <M> <M> miles <M>
	4	o <M> <M> air## <M> <M> has an an <M> of <M> square miles <M>
	5	o <M> this air## port alone has an an <M> of <M> square miles <M>
	6	o <M> this air## port alone has an an <M> of <M> square miles <M>
	7	o <M> this air## port alone has an an <M> of <M> square miles .
	8	o <M> this air## port alone has an an <M> of 100 square miles .
	9	o <M> this air## port alone has an an <M> of 100 square miles .
	10	o and this air## port alone has an an area of 100 square miles .
RDM-absorbing	0	o <M>
	1	o <M> <M> air## <M> <M> <M> <M> <M> <M> square <M> <M>
	2	o <M> <M> air## <M> <M> <M> <M> <M> <M> square <M> .
	3	o <M> <M> air## <M> alone <M> <M> area <M> 100 square kilometers .
	4	o <M> <M> air## port <M> <M> an <M> of <M> square kilometers .
	5	o <M> <M> air## <M> <M> <M> area of 100 square kilometers .
	6	o <M> this air## port <M> <M> an area of <M> square kilometers .
	7	o <M> this air## port alone <M> an area of 100 square kilometers .
	8	o <M> this air## port <M> has an area of 100 square kilometers .
	9	o <M> this air## port alone has an area of 100 square kilometers .
	10	o so this air## port alone has an area of 100 square kilometers .
Multinomial	0	o eher spending des## vagina drin production mili## inven## primi## open## freiheit sit schlüssel search
	1	o alone alone air## air## port has a a area of 100 square miles .
	2	o alone alone air## air## port has a a area of 100 square miles .
	3	o alone alone air## air## port has a a area of 100 square miles .
	4	o alone alone air## air## port has a a area of 100 square miles .
	5	o alone alone air## air## port has a a area of 100 square miles .
	6	o alone alone air## air## port has a a area of 100 square miles .
	7	o alone alone air## air## port has a a area of 100 square miles .
	8	o alone alone air## air## port has a a area of 100 square miles .
	9	o alone alone air## air## port has a a area of 100 square miles .
	10	o alone alone air## air## port has a a area of 100 square miles .
RDM-multinomial	0	o beschreiben denk## architect mittleren words alism grou## hilft atoms pus he## jähri## enti## ball## generally
	1	o expe## standing nahme cted baum katastrop## bares tion later colle## haufen 100 anstatt zy .
	2	o cognitive standing natürlich cted ution ity bares an later aus## informa## 100 square zy .
	3	o cognitive standing llig port wieder oth has an later erhalten saal 100 square kilometers .
	4	o crime standing air## port spending imag## has an area incredible of 100 square prototyp## .
	5	o crime standing air## port alone psychi## edi## an area oder of 100 square prototyp## .
	6	o starke standing air## port alone psychi## armut an area out of 100 square kilometers .
	7	o starke that air## port alone psychi## armut an area out of 100 square kilometers .
	8	o starke that air## port alone has armut an area out of 100 square kilometers .
	9	o and that air## port alone has got an area out of 100 square kilometers .
	10	o and that air## port alone has got an area out of 100 square kilometers .